Modelling Summertime Ozone in North China

Siyu Cheng

Lancaster Environment Centre

March 2020

This Dissertation is submitted in partial fulfilment of the degree of Master of Science by Research in Environmental Science.

This Dissertation is submitted in partial fulfilment of the degree of Master of Science by Research in Environmental Science. It is the candidate's own work and has not been submitted in substantially the same form for the award of a higher degree elsewhere.

Abstract

A high-resolution nested air quality model, the Weather Research and Forecasting (WRF) model coupled with Chemistry (WRF-Chem), was applied to simulate the ozone concentration in North China from 15 May 2017 to 22 June 2017 to investigate the appropriate emissions for the Atmospheric Pollution and Human Health in a Chinese Megacity (APHH-Beijing) programme campaign period and study an ozone pollution event at the end of May 2017. The model reproduced the meteorological parameters of temperature, relative humidity, wind speed and wind direction relatively well over the period. The key air pollutants of ozone, NO_x, SO_2, $PM_{2.5}$ and PM_{10} are captured reasonable well compared with observations. Results suggest that the ozone simulation matches the observation and simulations of NO_2 and SO_2 are generally satisfactory with emissions scaled down based on previous studies about anthropogenic emissions changes in China. The model underestimated the peaks of ozone concentration, especially in heavily polluted days, which remains a challenge for modelling ozone and may be attributed to the model's weakness of diurnal cycle of NO and different between concentration of simulated and observed VOC and isoprene. We carried out sensitivity studies investigating how NO_x, VOC and isoprene emissions changes affects the simulation of ozone, and improved the ozone simulation of the peaks with 50% increased VOC emissions and doubled isoprene emission. We speculate that the underestimation of VOC emissions or the reactivities of VOC in the model could be the reasons of underestimation of the peaks of ozone concentration and further investigation is needed to improve the simulation of ozone concentration. We also note that increasing isoprene emission factor can increase the isoprene concentration then improve simulation of ozone concentration, but the simulation on isoprene still can be improved, which lead to the need for investigations on isoprene emission and the processes of model's simulation on isoprene. This study discusses the simulation effects of different emissions, analyses the weakness of the model on simulating ozone and proposes the need for further research on VOC and isoprene simulations.

Keywords

Ozone concentration, WRF-Chem, anthropogenic emission, biogenic emission, emission changes

Contents

1. Introduction **1**

2. Model and measurements **5**

2.1 Model description 5

2.2 Emission inventories 7

2.3 Observation data 9

3. Results and discussion **11**

3.1 Model evaluation 11

3.2 Air quality simulation 15

3.2.1 Comparison over the full campaign period 15

3.2.2 Analyses of baseline run 19

3.2.3 Analyses of meteorology during high pollution period 21

4. Sensitivity studies for a pollution episode **24**

4.1 Independent emission changes 24

4.2 Best emissions scenario 30

5. Conclusion **33**

Figures in the article

Figure 1. Maps of the domains used in this study and locations of observation sites. 6

Figure 2. Comparison of observed and simulated meteorological parameters at ground level, 120 meters and 240 meters. 13

Figure 3. Mean spatial 24-hour ground level concentration of ozone from 15th May to 22nd June 2017 over domain 1 (China) and domain 3 (North China Plain). 16

Figure 4. Concentrations of O_3, NO, NO_2, SO_2, CO, aromatics and isoprene timeseries at IAP, Beijing. 20

Figure 5. Concentrations of Ozone and a) NO_x timeseries at IAP, Beijing with NO_x emissions increased and decreased by 50%; b) VOC timeseries at IAP, Beijing with VOC emissions increased and decreased by 50%; c) isoprene timeseries at IAP, Beijing with isoprene emission biogenic emissions doubled. 27

Figure 6. Concentrations of ozone, NO_2, NO, aromatics and isoprene timeseries at IAP, Beijing with VOC emissions increased by 50% and isoprene emissions factor in biogenic emissions doubled. 32

Tables in the article

Table 1. Model configuration used in this study. 5

Table 2. Emission inventories used in this study. 8

Table 3. Comparison of hourly observed and simulated meteorological parameters at ground level, 120 meters and 240 meters. 12

Table 4. Comparison of hourly observed and simulated air pollutants in three baseline runs at IAP and 12 sites in Beijing. 15

Table 5. Emission reductions by percentage for MEIC emissions used in second run based on the first run. 18

Table 6. Comparison of hourly observed and simulated meteorological parameters at ground level, 120 meters and 240 meters during a heavy ozone pollution period (22-29 May 2017). 23

Table 7. Changes in emissions by percentage applied to the baseline scenario (R2) for the sensitivity studies. 24

Table 8. Comparison of hourly observed and simulated air pollutants in baseline and sensitivity runs at IAP in Beijing during 22-29 May 2017. 25

Table 9. Comparison of hourly observed and simulated air pollutants in best guess sensitivity run and baseline run at IAP in Beijing during 22-29 May 2017. 31

1. Introduction

As one of the largest environmental risks, air pollution has significant impact on human health and ecosystems. Since air pollution in megacities in the 20th century has attracted the attention of researchers, the studies on air pollution has led to huge progress in understanding the sources and pollution processes in megacities in western countries. However, due to the rapid industrialisation and growth in the number of vehicles, serious air pollution problems are gradually emerging in fast-developing cities and has become more complex than the past.

With the fast development and rapid industrialisation in China, air pollution in megacities in China has become a topic of major concern in recent years. It is suggested that the $PM_{2.5}$ and ozone are the key air pollutants for megacities and its surrounding area in China, such as Beijing and North China. Although the emission restrictions have been taken to improve air quality and the concentration of $PM_{2.5}$ has been decreasing (Cheng et al., 2019; Li et al. 2019a), results from air quality measurement program in China show that the concentration of ozone has been increasing (Shi et al., 2019). Li et al. (2019a) reported a 1-3 ppbv a^{-1} increasing trend of ozone concentration in megacity clusters of eastern China, and indicated that North China Plain (NCP, with Beijing located in the northeast) is the most ozone pollution area in China based on the observations, where summertime MDA8 ozone is the highest over the NCP and the highest ozone concentration can reach 150 ppbv in summer. They noted that their simulation using GEOS-Chem model indicate the decreasing $PM_{2.5}$ in the NCP from 2013 to 2017 as a vital factor for ozone changes because it leads to the increase of hydroperoxy radicals (HO_2). Apart from increasing the mean concentration of ozone, the number of ozone pollution events in summertime is growing in recent years. It is suggested that the occurrence of severe ozone pollution days (MDA8 greater than 110 ppbv) in summer is increasing from 2014 to 2017 (Ma et al., 2019). Lyu et al. (2019) also reported a continuous O_3 pollution event during 4-11 August 2017 in Jinan, a city located in the central of NCP, with the highest hourly O_3 mixing ratio reaching 154.1 ppbv.

High concentrations of ozone can cause severe adverse impacts on human health and vegetation. Ozone is one of the risk factors for chronic obstructive pulmonary disease (COPD) (Soriano et al., 2017) and led to 254 000 (95% UI 97 000-422 000) deaths and 4.1 million (1.6

million to 6.8 million) disability-adjusted life-years (DALYs) globally in 2015 from COPD (Cohen et al., 2017). Besides, ozone pollution may lead to a yield loss of 5-20% for important crops in Asia, such as wheat, rice and Legumes (Emberson et al., 2009). Based on the market price for year 2000, an economic loss of $ 14-26 billion is estimated, translated by assumed yield loss in wheat, soybean, rice and maize due to surface ozone, and about 40% loss occurs in China and India (Van Dingenen et al., 2009). Therefore, it is vital to control the concentration of ozone and reduce ozone pollution.

Tropospheric ozone is closely related to meteorological conditions. Besides, tropospheric ozone is a secondary pollutant which concentration is highly related to the precursor pollutants such as volatile organic compounds (VOC) and nitrogen oxides (NOx, NOx = NO + NO2) emissions, which are important for photochemical reactions and ozone formation in the presence of sunlight (Brasseur et al., 1999; Xing et al., 2011). The main source of ozone in the troposphere is photochemical formation. In the presence of a sufficiently high mixing ratios of NO (≥10 pptv), HO_2 formed by the OH-initiated oxidation of VOC (e.g. hydrocarbons) converts NO to NO_2 (Wallace et al., 2006; Lyu et al., 2019). Then O_3 is produced followed by:

$$RH + OH + O_2 \rightarrow RO_2 + H_2O,$$

$$RO_2 + NO \rightarrow RO + NO_2,$$

$$NO_2 + h\nu \xrightarrow{O_2} NO + O3$$

Besides, NO can catalyse the removal of ozone:

$$NO + O_3 \rightarrow NO_2 + O_2$$

As NO can be involved in both the production of ozone and promote its removal when the NO + O_3 reaction is competitive (e.g. when the NO concentration is high), the production of tropospheric O_3 is mainly determined by reactions that compete with NO + O_3 for NO, such as HO_2, CH_3O_2, and other RO_2. It should be mentioned that, when NO concentration is high enough, the excess NO will participate in the above ozone removal reaction, which means high NO concentration can titrate ozone .Among them, NO + HO_2 and NO + CH_3O_2 (from methane oxidation) are the main sources of troposphere O_3 (Jacob, 1999). Therefore, the concentration of ozone is generally limited by VOC or NOx or co-limited by both of them,

which depends on the chemical composition of the air, particularly the ratio between the reactivity of OH (the sum of the products of O_3 precursor concentrations and the reaction rate constants between O_3 precursors and OH) with VOCs and NOx (Wallace et al., 2006).

It is suggested that the anthropogenic NOx emissions decreased during 2013–2017, both in Beijing and its surrounding area (Cheng et al., 2019) and in China (Li et al., 2019a; Zheng et al., 2018). The changes of VOC emissions are less well understood than NO_x because many species are included and the balance between them also changes with time, so that the in-depth research on VOC emission changes in recent decade is more complex. For anthropogenic VOC emissions such as alkanes, aromatics, studies suggest that the total VOC emissions decreased in Beijing but changed little in surrounding area (Cheng et al., 2019). However, although the emissions reductions have been evaluated to be effective of China's Clean Air Action since 2013, the concentration of ozone is still not well controlled, especially in summertime, and our understanding of sources of pollutants and atmospheric processing is still not completed (Shi et al., 2019.). These facts indicate a strong need for further research on ozone pollution in north China.

In order to improve the understanding of sources and formation processes of key air pollutants in China, the jointly organised China-UK Atmospheric Pollution and Human Health in a Chinese Megacity (APHH-Beijing) programme provided observations of air quality in Beijing (Shi et al., 2019). As a part of APHH-Beijing project, this research uses an air quality model to discuss sources and changes of ozone in China, aiming at analysing ozone pollution in China, mainly focusing on North China, through this modelling study.

In this study, we investigate the ozone problem by modelling summertime ozone over North China from 15 May to 22 June in 2017 using the Weather Research and Forecasting (WRF) model coupled with Chemistry (WRF-Chem). As the APHH-Beijing project offers continuously reliable hourly observations on both meteorology and air quality during this campaign period (Shi et al., 2019), we will compare the observations with the simulated meteorological parameters and concentrations of air pollutants obtained by running WRF-Chem model. WRF-Chem has been successfully used to investigate the $PM_{2.5}$ pollution in China (Zhang et al., 2013; Wang et al., 2014; Guo et al., 2016; Zhang et al., 2015) and the ozone

pollution in many other cities over the world (Tuccella et al., 2012; Safieddine et al., 2014; Bao et al., 2008; Tie et al., 2007, 2010; Geng et al., 2007; Tie et al., 2009, 2013). We evaluate the performance of the model in North China and investigate the performance of the model with different anthropogenic emissions on simulating ozone concentrations. Noting that the performance of the model can be improved especially during an ozone pollution event in late May 2017, we then carry out sensitivity studies on how to improve the emissions and improve the simulation of ozone during the ozone pollution period by adjusting the emissions, aiming to improve our understanding of ozone pollution and raise the possibilities on improving the existing emissions.

2. Model and Measurements

2.1 Model description

To simulate the ozone concentration and analyse the relations between ozone concentration ozone in the troposphere and the emission changes, we apply the WRF-Chem model (version 3.7.1) which is used for investigating regional-scale air quality (Grell et al., 2005; Fast et al., 2006). The WRF-Chem model is a high-resolution nested air quality model which simulates the processes controlling pollutants (emissions, transport, mixing and chemical transformations, etc.) under the prevailing meteorological conditions. This modelling system can be applicated into simulating weather, climate and air quality. Previous studies have shown that WRF-Chem model can reproduce air quality in China (Tie et al., 2009; Zhang et al., 2013; Wang et al., 2014; Zhang et al., 2015; Guo et al., 2016; Ma et al., 2019). The simulation results of this model can match the observation level and the changes during the simulation period can be captured. Most of previous studies using WRF-Chem to investigate air pollution in China focus on $PM_{2.5}$ (Zhang et al., 2013; Wang et al., 2014; Zhang et al., 2015; Guo et al., 2016), with previous experiences on using WRF-Chem to investigate ozone issues in Europe (Tuccella et al., 2012; Safieddine et al., 2014;), America (Bao et al., 2008; Tie et al., 2007, 2010) and Southern China (Geng et al., 2007; Tie et al., 2009, 2013).

Table 1. Model configuration used in this study.

Horizontal resolutions	27km, 9km, 3km
Vertical layers	31 layers, 50 hPa at top
Aerosol scheme	MOSAIC with eight bins
Gas-phase chemistry	CBMZ
Meteorology	FNL
Chemical boundary conditions	MOZART
Anthropogenic emissions	MEIC 2010
Biogenic emissions	MEGAN
Fire emissions	FINN

Table 1 introduces the model configuration used in this study, which has been shown to perform well for simulating $PM_{2.5}$ in a previous study (Ansari et al., 2019). The meteorological conditions we used are 6-hourly NCEP FNL Operational Global Analysis data with a resolution of 1° × 1°. We also use the Yonsei University PBL (YSU PBL) boundary layers to reproduce the meteorological conditions within the planetary boundary layer (Hong et al., 2006), the NOAH Land Surface Model (Chen and Dudhia., 2001), the Rapid Radiative Transfer Model for GCMs (RRTMG) longwave and shortwave scheme and Grell 3-D cumulus scheme.

Figure 1 shows the three domains of simulation used in this study. These three domains are set for modelling ozone over China, northern China and North China Plain on a Lambert map projection, which resolutions of three domains are 27km, 9km, 3km, respectively. Vertically, the model has 31 layers and top pressure at 50 hPa. To simulate atmospheric chemistry, the Carbon Bond Mechanism version Z (CBMZ) chemistry scheme and FAST-J photolysis scheme are used in this study. Chemical boundary conditions are from Model for Ozone and Related chemical Tracers (MOZART).

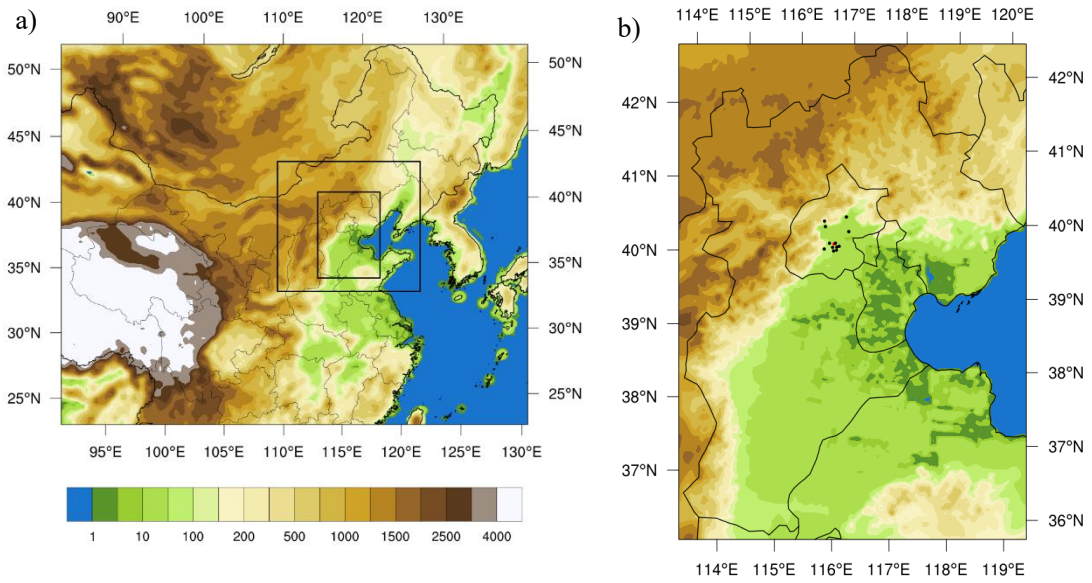

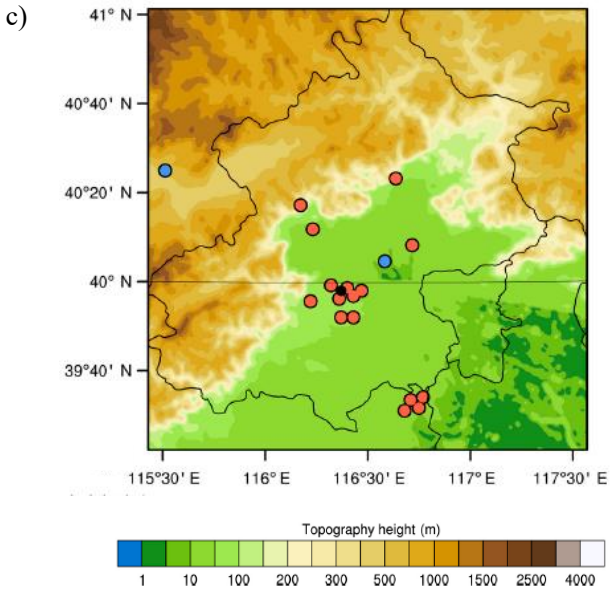

Figure 1. Maps of the domains used in this study: a) domain 1 with domain 2 and 3 marked on the picture; b) domain 3 with the locations of the Institute of Atmospheric Physics meteorological tower site in central Beijing (red point) and 12 sites of national monitoring networks (black points) and; c) the Beijing region with locations of IAP site (red point) and 12 sites of national monitoring networks (black points).

2.2 Emission inventories

The anthropogenic emissions we used are from the Multi-resolution Emission Inventory for China (MEIC) for the year 2010 and 2013 redistributed to 2017, which is a bottom up anthropogenic emissions inventories for air pollutants and greenhouse gases developed by Tsinghua University and have been used in previous modelling studies (Hu et al., 2016; Cheng et al., 2019; Ansari et al., 2019). MEIC provide emissions of 10 major atmospheric pollutants and greenhouse gases including SO_2, NO_x, CO, non-methane volatile organic compounds (NMVOC), $PM_{2.5}$ and PM_{10} (Li et al., 2017). Emissions were provided at 27 km, 9 km and 3km, which are the same resolutions of each domain.

Table 2. Emission inventories used in this study.

	Anthropogenic emission	Biogenic emission	Fire emission
Run 1	MEIC 2010 scaled to 2014	MEGAN	Turned off
Run 2	MEIC 2010 rescaled to 2017	MEGAN	FINN
Run 3	MEIC 2013 redistributed to 2017	MEGAN	FINN

In 2010, China has implemented the clean air policies to control the emissions of major air pollutants. Previous studies have indicated the emission changes in recent years caused by the clean air actions (Zheng et al., 2018; Cheng et al., 2019). In this study, we ran three full-period (from 15 May to 22 June 2017) simulations using different anthropogenic emissions in order to evaluate these anthropogenic emissions for modelling summertime ozone in 2017. The anthropogenic emissions we used in these three full-period runs are listed in Table 2. In the first run, we used the emissions for modelling air quality in 2014. In the second run, emissions over north China plain were rescaled to 2017 to represent the emission reductions. Based on the concentration difference of the chemicals between simulation results in the first run and the observed values combined with studies on emission changes in China, SO_2 emissions were reduced by 55% over Northern China (domain 2) and 70% over North China Plain (domain 3). Emissions of NO_x were reduced by 20% over Northern China (domain 2) and 35% over North China Plain (domain 3). $PM_{2.5}$ emissions were reduced by 15% over Northern China (domain 2) and 25% over North China Plain (domain 3). Emissions of VOC were reduced by 35% over North China Plain (domain 3) (Zheng et al., 2018; Cheng et al., 2019; Ansari et al., 2019). In addition, a MEIC emissions redistributed from MEIC 2013 offered by collaborators at the Institute of Atmospheric Physics (IAP) of the Chinese Academy of Sciences in Beijing were also used in our runs and compare the results with observation and other runs with scaled emissions.

For biogenic emissions, the online calculation from Model of Emissions of Gases and

Aerosols from Nature version 2.1 (MEGAN) is used in this study. This is a total of emissions of 150 chemical species including isoprene emission factor. Isoprene emission factor ($\mu g \cdot m^{-2} \cdot hr^{-1}$) is using for calculating isoprene emission which is important in ozone formation. Fire emissions ar from the Fire Emissions INventory from NCAR (FINN) based on satellite observations (Wiedinmyer et al., 2011), which is included in the second and third full-period run.

2.3 Observation data

As meteorological conditions influence the processes controlling pollutants, and tropospheric ozone is also closely related to meteorological conditions and precursor pollutants such as nitrogen oxides NOx and volatile organic compounds (VOCs), evaluations are therefore needed to ensure that the model is reliable in simulation of weather conditions and atmospheric pollutants by comparing the modelling results with the observations. As the Atmospheric Pollution and Human Health in a Chinese Megacity (APHH-Beijing) programme, which is an international collaborative project between research groups from China and UK, focusing on understanding the sources, processes and health effects of air pollution in the Beijing megacity, can provide continuously reliable hourly observations on both meteorology and air quality from 15 May to 22 June 2017 (Shi et al., 2019), we set the simulated time period starting from 15 May 2017 and ending on 22 June 2017, which covers the observed campaign period from APHH-Beijing programme.

To evaluate the model, the observations from both the Institute of Atmospheric Physics (IAP) meteorological tower site in central Beijing and national monitoring networks run by the China National Environmental Monitoring Center (CNEMC) were used to compare with the meteorological modelling results. Figure 1c shows the locations of IAP tower (black point) and 12 monitoring sites (red points) in Beijing. For meteorological variables, observations we used are from the 325-metre-tall tower for meteorological measurements located at the Institute of Atmospheric Physics (IAP), Chinese Academy of Sciences, Beijing (39°58'28"N, 116°22'16"E). The measurements we use are temperature, relative humidity, wind speed, and wind direction at 8 meters, 120 meters and 240 meters at this site. For atmospheric pollutants, measurements from IAP tower we used provides hourly concentration of ozone, SO_2, NO, NO_2, CO, aromatics

and isoprene at ground level. The observations from national monitoring networks run by the China National Environmental Monitoring Center (CNEMC) are also available, which includes concentrations of ozone, SO_2, NO_2, CO, $PM_{2.5}$ and PM_{10} at 12 different locations in both urban and rural area in Beijing.

3. Results and discussion

To investigate the air quality in summer 2017 using WRF-Chem model, the simulations were set to start running from 13 May 2017. The first 2 days are set as spin-up time so the results for analysing are starting from 15 May 2017, ending on 22 June 2017, which is the same as the ending time of the observations. Observed meteorological data from three different heights of the Institute of Atmospheric Physics (IAP) meteorological tower site in central Beijing and air pollutants measurements from both IAP tower site and 12 sites of national monitoring networks are used for evaluating the performance of the model in the simulation period.

3.1 Model evaluation

We evaluate the model performance on reproducing the meteorological variables by using the observed meteorological data from IAP. The comparison contains temperature, relative humidity, wind speed and wind direction at three different levels: 8m, 120m and 240m.

Table 3 presents a comparison of model performance and observations on each level. In table:

Sim. Avg. is the average of the model's simulation results;

Obs. Avg. is the average of observation data;

Bias = Sim. Avg - Obs. Avg. , reflecting the difference between the simulation results and observation data;

$\mathrm{RMSE} = \sqrt{\frac{\sum_{i=1}^{n}(\mathrm{Sim}._i - Obs._i)^2}{\mathrm{n}}}$, n is the sample size. RMSE is used to measure the deviation between the simulated and observed value.;

$r = \frac{\sum_{i=1}^{n}(Sim._i - Sim.Avg.)\cdot(Obs._i - Obs.Avg.)}{\sigma_{Sim.}\cdot\sigma_{Avg.}}$, n is the sample size, $\sigma_{\mathrm{Sim.}}$ and $\sigma_{\mathrm{Avg.}}$ are the standard deviations of simulation and observation results. Correlation reflects the level of linear correlation between simulation and observation.

Table 3 suggests that the ground-level temperature is well reproduced by the model as the difference between mean value and the deviation are small (Bias = 0.21, RMSE = 2.00 at ground level). At 120m and 240m, the model begins to overestimate the temperature as the simulations of the average temperature are almost the same as the near-ground level while the observations decreased and the bias increased (Bias = 1.81 at 120m, =3.13 at 240m) , which is probably

because the levels in the model are too well mixed. As the model overestimated the temperature, the simulated average relative humidity is systematically underpredicted by about 15% at near-ground level and about 10% at 120m and 240m, which matches the results of previous study (Ansari et al., 2019). We suggest that the underestimation of relative humidity may be a consequence of the overestimation of temperature due to the strong dependence of saturation vapour pressure and hence relative humidity. The humidity at the near-ground level is more underestimated than upper levels as the bias is greatest at the surface (Bias=-18.54 at ground level), which may be attributed to the inappropriate land surface and vegetation in central Beijing. The bias is expected as the model does not reproduce the urban canopy (the heating and friction at the surface). For simulations of the wind, the model performs better at upper levels than near-ground level. At ground level the model is not able to reproduce the measurements well, mainly because of the impact of surface constructions. At upper levels, the wind speed and direction can be captured in general, showing significant improvements on correlations of wind speed and wind direction because they are not affected by the buildings on the surface.

Table 3. Comparison of hourly observed and simulated meteorological parameters at ground level, 120 meters and 240 meters during campaign period (15 May – 22 June 2017).

		Obs. Avg.	Sim. Avg.	Bias	RMSE	r
Temperature (°C)	**8m**	26.91	27.12	0.21	2.00	0.94
	120m	25.29	27.10	1.81	2.78	0.94
	240m	24.19	27.32	3.13	3.83	0.94
RH (%)	**8m**	48.58	30.04	-18.54	21.48	0.84
	120m	43.58	32.25	-11.33	15.02	0.87
	240m	44.90	33.97	-10.93	14.75	0.87
Wind Speed (m/s)	**8m**	1.28	3.49	2.21	2.92	0.24
	120m	3.55	4.67	1.12	2.54	0.60
	240m	4.70	5.11	0.41	2.61	0.64

	8m	160.9	165.4	4.5	78.10	0.58
Wind Direction	**120m**	160.4	171.2	10.8	69.52	0.64
(°)	**240m**	168.6	174.8	6.2	60.38	0.76

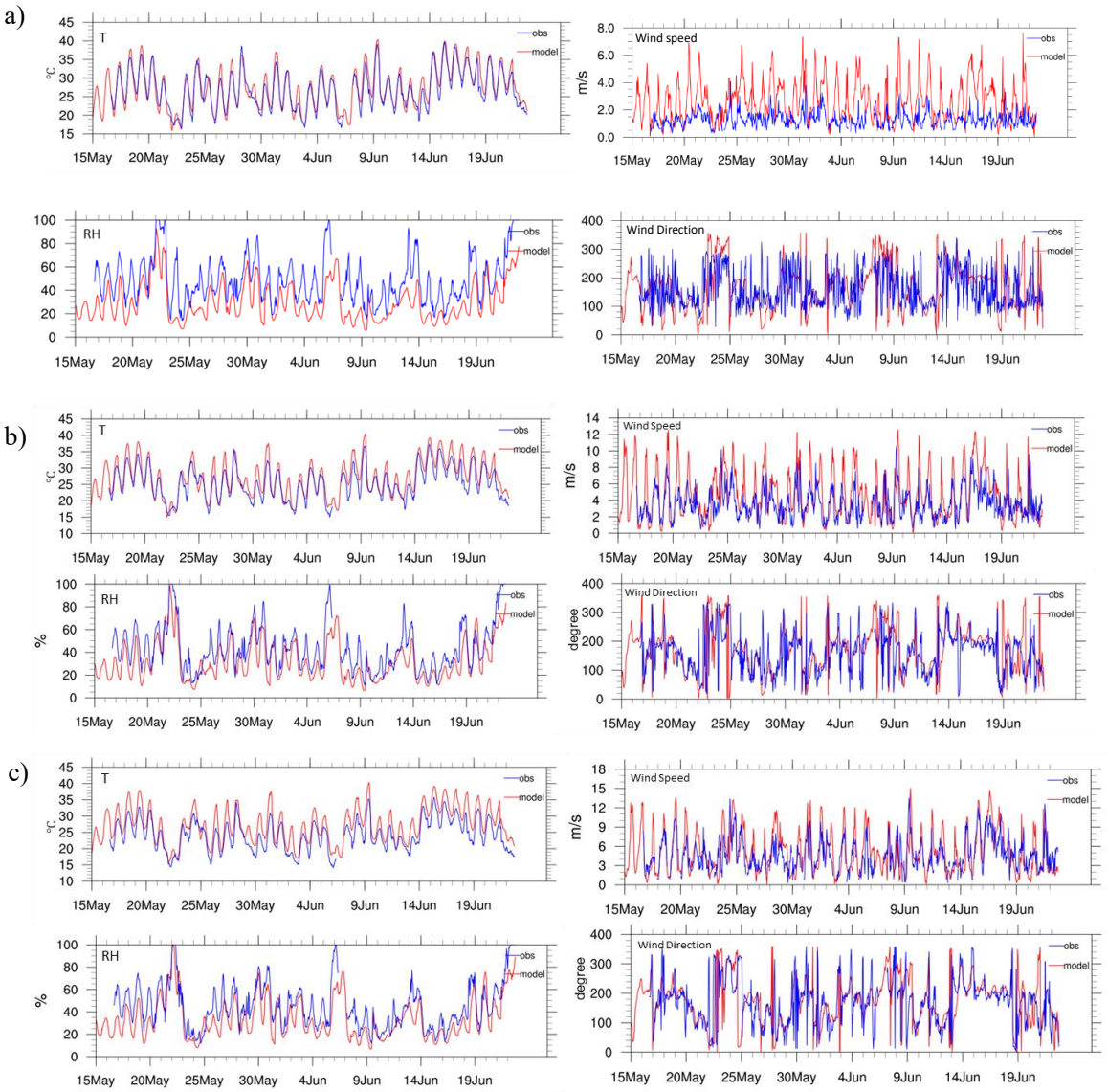

Figure 2. Comparison of observed and simulated meteorological parameters hourly: a) Temperature, Relative Humidity, Wind Speed and Wind Direction timeseries at Ground Level; b) Temperature, Relative Humidity, Wind Speed and Wind Direction timeseries at 120m, and c) Temperature, Relative Humidity, Wind Speed and Wind Direction timeseries at 240m.

Figure 2 shows the timeseries of hourly observed and simulated meteorological variables at

ground level, 120 metres and 240 metres at IAP tower in Beijing from 15th May to 22nd June 2017. Generally, we note that there is a general warming over this period. A short cold period with high relative humidity occurred around 23 May 2017, and two short periods of relatively slow wind from relatively steady direction around 26 to 28 May 2017 and 15 to 18 June 2017. These two short periods of low wind speed and steady wind directions may explain the accumulation of pollutants in the air during these periods.

Comparing the simulations with the observations, we note that the model can capture the same daily variation as observations when simulating the temperature. The model begins to overestimate the peaks and the minima at 120m and 240m and the relative humidity is therefore underpredicted. But the model still can capture all the peaks and dips at the same timepoints as the observations in the campaign period. When simulating the wind, the model captures the variations of wind speed and changes of wind variation with a significant underestimation of peaks of wind speed and some variation of wind directions. Overall, the meteorological parameters can be reproduced relatively well. The model captures the mean level of meteorological parameters (Bias = 0.21 for temperature at ground level, 10%-15% for RH, = 0.41 for wind speed and ≤10° for wind direction at upper level). The diurnal cycle of temperature is well reproduced (r = 0.94 at all three level), and variations of RH, wind speed and wind direction are captured (correlations at three levels are about 0.85 for RH, at upper levels are about 0.6 for wind speed and 0.6-0.7 for wind direction).

3.2 Air quality simulations

3.2.1 Comparison over the full campaign period

Table 4. Comparison of hourly observed and simulated concentration of chemicals in three runs at IAP and 12 sites in Beijing (domain 3).

	Obs.	Sim. Avg.			Bias			RMSE			r		
	Avg.	R1	R2	R3	R1	R2	R3	R1	R2	R3	R1	R2	R3
O_3 (ppbv)													
IAP	55.74	37.91	45.54	66.78	-17.83	-10.19	11.03	32.99	28.74	30.32	0.65	0.68	0.66
12 sites	53.82	44.86	50.73	65.89	-8.95	-3.07	12.07	23.91	21.86	26.59	0.72	0.74	0.69
NO_2 (ppbv)													
IAP	21.57	36.26	25.77	9.83	14.70	4.20	-11.73	23.51	16.83	17.81	0.26	0.28	0.30
12 sites	18.32	27.08	18.91	8.59	8.76	0.58	-9.73	13.73	8.71	12.67	0.41	0.44	0.35
NO (ppbv)													
IAP	4.60	10.42	4.53	0.54	5.82	-0.07	-4.05	19.02	11.80	11.12	0.22	0.21	0.25
SO_2 (ppbv)													
IAP	2.58	8.05	1.80	3.67	5.48	-0.77	1.10	7.06	2.78	3.63	0.07	0.08	-0.05
12 sites	2.72	6.40	1.56	2.92	3.68	-1.15	0.19	4.76	2.45	2.38	0.19	0.22	0.12
CO (ppbv)													
IAP	545.5	639.3	638.5	621.0	93.83	93.04	75.55	335.2	333.0	320.0	0.26	0.26	0.27
12 sites	585.6	587.6	586.6	565.7	2.03	1.03	-19.86	268.0	267.4	259.4	0.29	0.29	0.31
Aromatics (ppbv)													
IAP	0.48	-	6.42	11.87	-	5.94	11.40	-	7.11	13.85	-	0.07	0.08
$PM_{2.5}$ (μg/m3)													
12 sites	44.38	48.10	42.65	42.44	3.72	-1.73	-1.93	21.56	20.68	24.20	0.60	0.59	0.50
PM_{10} (μg/m3)													
12 sites	87.82	53.40	48.02	47.87	-34.41	-39.79	-39.94	49.64	53.36	56.32	0.46	0.45	0.33

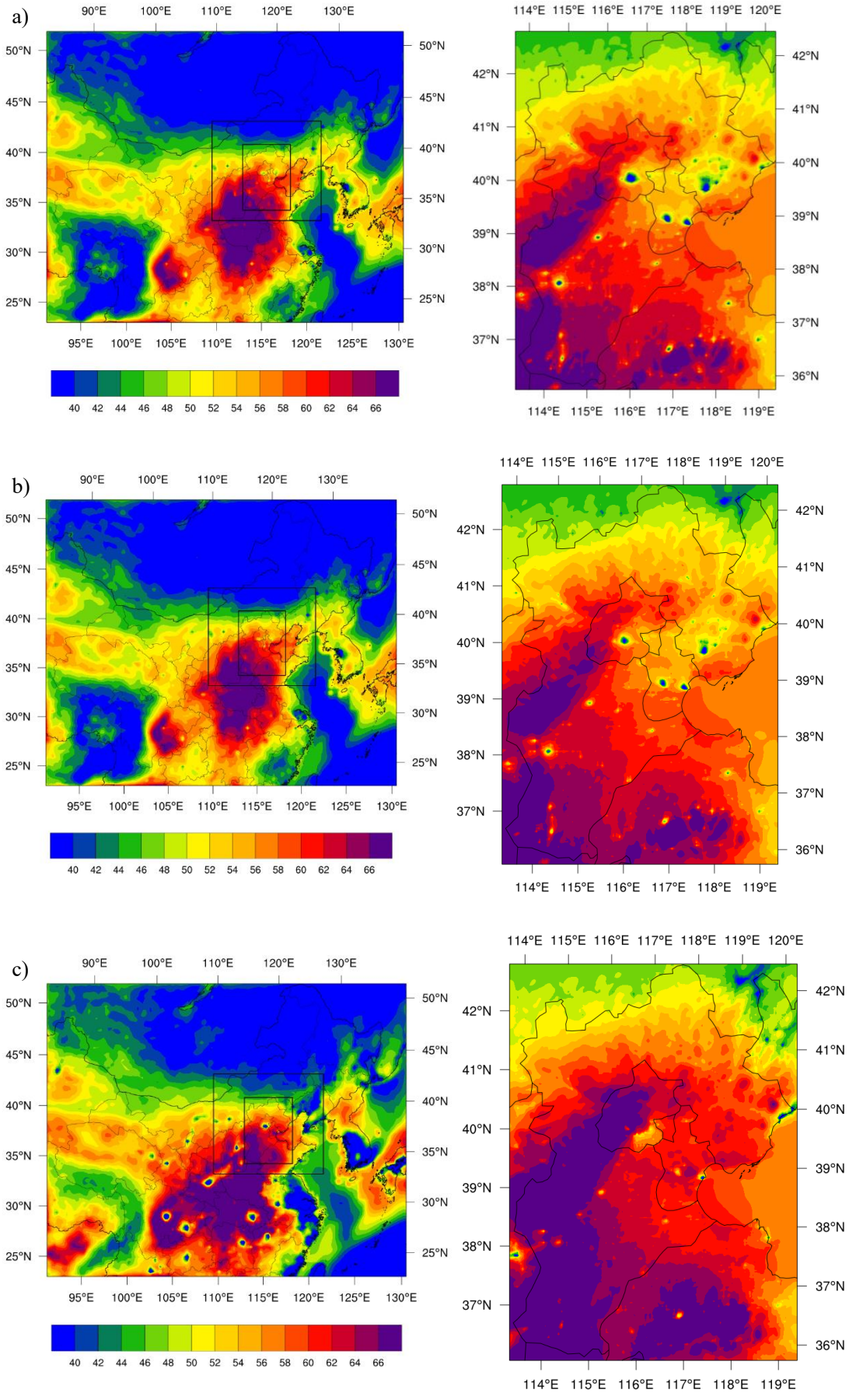
a)
b)
c)
90°E 100°E 110°E 120°E 130°E
50°N 45°N 40°N 35°N 30°N 25°N
95°E 100°E 105°E 110°E 115°E 120°E 125°E 130°E
40 42 44 46 48 50 52 54 56 58 60 62 64 66
114°E 115°E 116°E 117°E 118°E 119°E 120°E
42°N 41°N 40°N 39°N 38°N 37°N 36°N

Figure 3. Mean spatial 24-hour ground level concentration of ozone from 15th May to 22nd June 2017 over domain 1 (China) and domain 3 (North China Plain) in a) run1; b) run2; c) run3. (Units: ppbv)

Table 4 presents a comparison of hourly modelled pollutants for Beijing against observations at IAP and 12 sites from national monitoring networks (referred to as "12 sites" in the following). It is suggested that the bias at national monitoring sites are smaller than that at IAP in most cases, and the correlations are also improved. This suggests that the comparisons using the average of air pollutants of the 12 sites in Beijing are more regionally-representative over Beijing, while the deviations of air pollutants are greater when comparing between the model and the observations from the IAP site.

However, even though there are some differences of bias and correlations between IAP and the 12 sites, the comparisons of simulation results between these three full-period simulations from 15 May to 22 June using different anthropogenic emissions are the same at both IAP and the 12 sites. In the first run (R1), we used the anthropogenic emissions for modelling air quality in 2014, which is at the stage that emissions are just starting to decrease due to the efforts of clean air actions. Therefore, the NO_x and SO_2 concentrations are all overestimated by the model compared with observations. As simulated NO_x is too high, it inhibits the photodissociation of NO_2 and then the formation of ozone. Therefore, we applied the rescaled anthropogenic emissions based on studies of emissions changes in China (Zheng et al., 2018; Cheng et al., 2019) in the second run (R2). Table 5 summarizes the percentage of emissions reductions of anthropogenic emissions used in the second run (R2). The reductions in domain 3 reflect the emission changes in Beijing and reductions in domain 2 reflect the emission changes in the area surrounding Beijing from 2014 to 2017. Results suggest that the simulation of ozone is improved and simulations of NO_2 and SO_2 are generally satisfactory, as the bias decreased (Bias = -17.83 in run1, =-10.19 in run2 at IAP, =-8.95 in run1, =-3.07 in run2 at 12-site), and correlations are improved (r = 0.65 in run1, =-0.68 in run2 at IAP, =-0.72 in run1, =-0.74 in run2 at 12-site). This confirms the reductions we made to emissions based on previous related studies are reasonable and effective. The comparation of Figure 3a and Figure 3b also suggest that, the average concentrations of ozone increase in run2 compared with run1. We can note

that especially on some spots where high NO concentration titrating ozone, which can suggest that the NO concentration in run2 is lower than run1 so that the removal of ozone is reduced and hence the ozone concentration increases. In addition, we note that SO_2 simulation has significant improvement, which suggests that the use of coal has been reduced greatly during these years and provides strong support for the scaling applied in the second run (R2). These improvements of simulating concentration suggest that the second run with rescaled emissions is the most appropriate for modelling summertime ozone in 2017.

Table 5. Emission reductions by percentage for MEIC emissions used in second run relative to the first run.

	Northern China (Domain 2)	**Beijing (Domain 3)**
SO_2	55%	70%
NO_x	20%	35%
$PM_{2.5}$	15%	25%
VOC	-	35%

In addition, we carried out a third run which uses the emissions redistributed from MEIC 2013 provided by collaborators at the Institute of Atmospheric Physics (IAP) of the Chinese Academy of Sciences in Beijing. Figure 3b and 3c suggest that the simulated ozone concentrations over the domains are higher than run2. Compared with the observations, the ozone concentration is overestimated in run3 (Bias = 11.03 at IAP, =12.07 at 12-site). We note that the NO_x appeared to be too low in run3. This may be attributed to the redistribution of source of emissions in this anthropogenic emission. As the concentration of NO_x decreased, the removal of ozone with NO_x as reactants at night-time is suppressed. Therefore, ozone concentration in night-time is overestimated, when ozone should reduce to nearly 0 as the NO_x increased at night.

The correlations reflect whether the model can capture the variability of pollutant concentration well. Generally, we note that the variability is captured well for some species like ozone, for which the variability is driven by the diurnal cycle, but poorly for others. The

captured variability of NO_x is poor, suggesting that the model cannot always capture the spikes. CO is particularly poor given that it is largely a primary pollutant, suggesting that there are spatial and temporal emissions spikes which are not represented adequately. Comparing these three full-period runs, results show that the correlations of ozone, NO_x and SO_2 improve from R1 to R2, and drop for the third run (R3), which illustrates that the performance of the model in R2 is the best on capturing the variability of pollutants.

Considering the above results, we chose the second run as the baseline of this study as the ozone, NO_x and SO_2 simulation match the observations the best. We suggest that the emissions rescaled to 2017 are more appropriate than the emissions redistributed to 2017. In the redistributed emissions, the redistribution only changes the location of the emission sources so that the total amount of the emissions remains unchanged compared with 2013 , while the emissions are proved to be reduced from 2013 to 2017.

3.2.2 Analyses of baseline run

As we have found the best anthropogenic emissions for simulating summertime ozone in 2017 and selected the baseline run, mean spatial ground level 24-hour concentration of ozone from 15th May to 22nd June 2017 is shown in Figure 3b, which introduce the general regional distribution of mean ozone concentration over the China domain (domain 1; left) and the North China Plain (domain 3; right). Over the China domain, the maximum mean concentration of ozone during the campaign period reached 66ppbv, which appears in northern China and in the north of Central China. We also note that high values also occur over Sichuan, with low values out to the West and in the coastal Southeast. Figure 3b shows the mean concentration of ozone over North China Plain. The mean concentration of 24-hour ozone in most parts of the NCP has reached 50 ppbv. The maximum appears in the south of NCP, and gradually decreased from south to north. This may be attributed to the fact that coastal regions are more affected by onshore flow, and air flow may push the polluted air against the mountains to the west of the NCP. Figure 3b also suggests that more of local scale features over the major cities are shown over the NCP domain. The average concentrations of ozone on some small spots located in major cities, such as Beijing, Tianjin, etc. where NO emissions are strongest, are significantly lower than the surrounding. It suggests the high NO emissions located at the spots thus titrating

the local ozone as high NO concentrations lead to direct ozone removal.

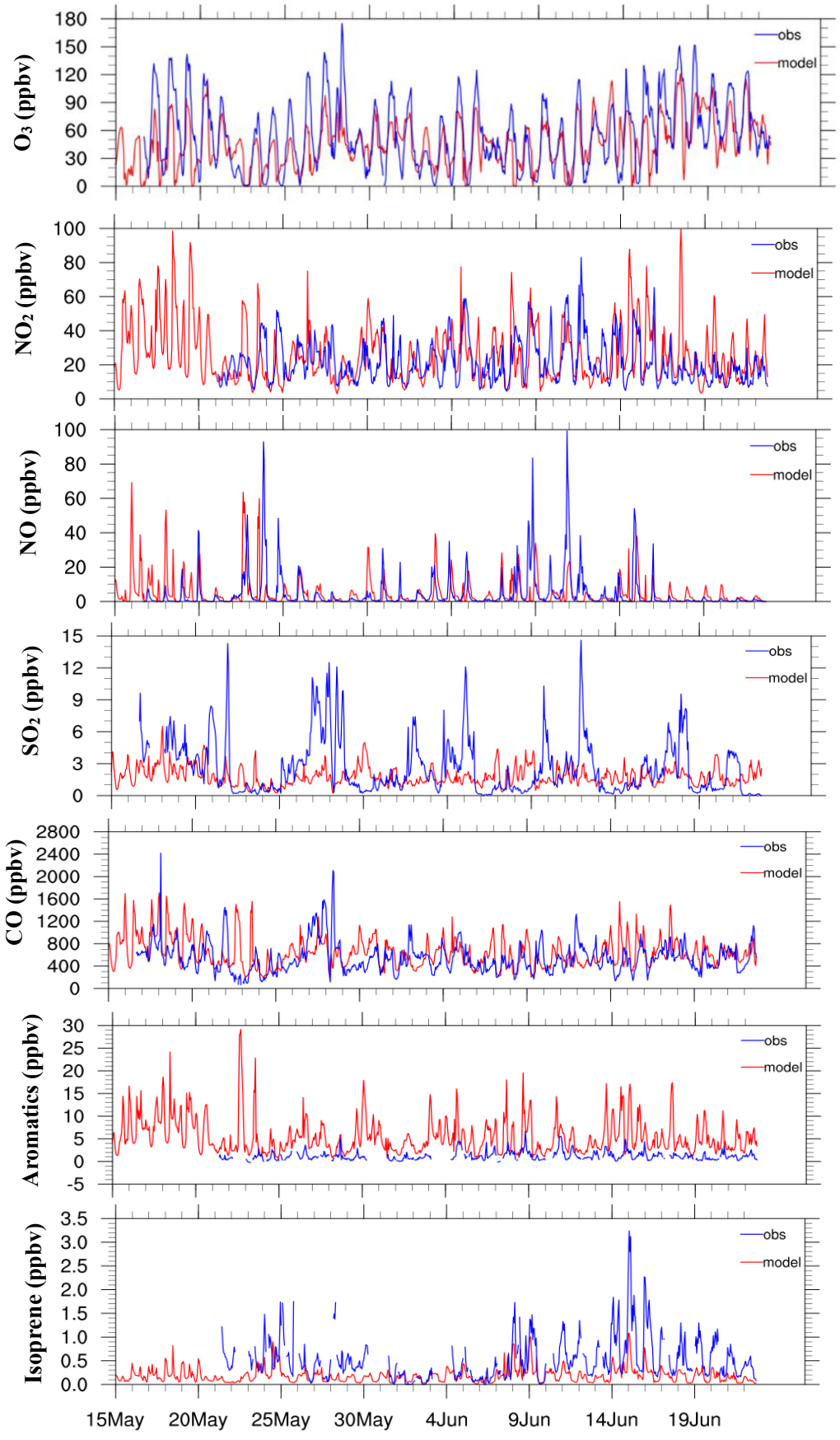

Figure 4. Concentrations of O_3, NO, NO_2, SO_2, CO, aromatics and isoprene timeseries at IAP,

Beijing.

To further evaluate the model, we analyse the hourly concentration timeseries of comparisons between simulations and observations. Figure 4 shows observed chemical variables and results of baseline run at IAP tower in Beijing from 15 May to 22 June 2017. We notice that the model can usually capture the daily variations for ozone and NO_2, but underestimates the peaks of ozone concentration in daytime when ozone produces under sunlight and the concentration increase. Efforts can be taken on improving the simulations of the peaks for ozone, which are usually underestimated in the model. For VOC, we compared the total concentration of aromatics in the model with the sum of observed concentrations of benzene, toluene, C_2-benzenes and C_3-benzenes (the observation did not include other aromatics). The results show that the model overestimated the concentration of aromatics. We suppose the simulated concentrations should be higher than the observations because not all the species of aromatics are included in the observations. The aromatics are lumped together in the model as representative species, but they are measured individually when observed. Results show that aldehydes are underestimated by the model comparing with observations of acetaldehyde, and ketones are also underestimated comparing with observations of methyl ethyl ketone and acetone. This suggests that some aromatics may be incorrectly simulated to other species of VOC by the model and cause the overestimation. For isoprene, the model underestimated its concentration. We suggest that it is because the land surface and vegetation may not be appropriate for central Beijing, as the emission of isoprene is highly related to vegetation. Also, Beijing has quite high tree coverage which contribute to the emission of isoprene, which have also been found underestimated in other studies (Naeem et al., 2018; Chen et al., 2018b; Zhao et al., 2019).

3.2.3 Analyses of meteorology during high pollution period

Further analysing the changes in ozone concentration during the whole campaign period, we note that there is an ozone pollution build-up and then heavily polluted period from 22 May to 29 May 2017, and the underestimation of ozone concentration in daytime is more significant during this period. In order to further improve the performance of the model in simulating ozone, we chose this period to carry out sensitivity studies. As meteorological conditions and emissions changes of NOx and VOC can both affect ozone concentration, we

therefore evaluate the model's performance on meteorology and compare the meteorological parameters during this polluted period with the whole campaign period. Results are summarized and shown in Table 6. We suggest that the average of simulation during the polluted period is very close to the whole campaign period, with a variation of about 1% on RH, 0.1m/s on wind speed and 10 degree on wind direction. The temperature has a variation of 1.5-2° C, which is reasonable considering the seasonal changes in Beijing. Compared with Table 3, the performance of the model during the polluted period also shows no significant difference compared on temperature and RH with the whole campaign period. When simulating the wind speed and wind direction, the dispersion and correlation of the model simulation results have been reduced. Considering the smaller amount of data during the pollution period (216 hours for the pollution period, 930 hours for the whole campaign period, where the model simulates every hour), we think that the difference on RMSE and correlations are acceptable. Overall, we suggest that the model's performance during the ozone pollution period it not significantly different from that over the whole campaign period. Therefore, we will focus on changing emissions to improve ozone simulation.

As ozone is a secondary pollutant, its concentration is closely related to emissions and concentrations of other atmospheric pollutants such as VOC and NO_x. Considering that improvements still can be made in emissions we used in baseline run, we carried out sensitivity studies in which the relationship between ozone and VOC/NO_x were further discussed.

Table 6. Comparison of hourly observed and simulated meteorological parameters at ground level, 120 meters and 240 meters during a heavy ozone pollution period (22-29 May 2017).

		Obs. Avg.	Sim. Avg.	Bias	RMSE	r
Temperature (°C)	**8m**	25.36	25.11	-0.25	2.03	0.92
	120m	23.87	25.12	1.25	2.27	0.93
	240m	22.86	25.44	2.58	3.23	0.92
RH (%)	**8m**	49.86	31.53	-18.33	21.21	0.87
	120m	44.18	33.48	-10.70	14.43	0.89
	240m	44.03	34.85	-9.18	13.89	0.87
Wind Speed (m/s)	**8m**	1.34	3.55	2.21	2.82	0.20
	120m	3.54	4.85	1.31	2.57	0.50
	240m	4.67	5.39	0.72	2.81	0.56
Wind Direction (°)	**8m**	168.18	163.41	-4.77	92.80	0.44
	120m	162.35	157.80	-4.55	103.97	0.40
	240m	167.23	164.81	-2.42	114.10	0.34

4. Sensitivity studies for a pollution episode

To investigate the relationship between ozone concentration and VOC/NO_x emissions and improve the model's performance in simulating ozone, we carried out sensitivity studies by changing the emissions to reproduce an ozone pollution period to analyse the influence of emission changes. We chose 21 May to 29 May as the campaign period for sensitivity studies with the first day set aside as spin-up. Figure 4 suggests that, during this period, observation showed the development and recovery of an ozone pollution event. This heavily polluted period is particularly poorly modelled, and therefore it is particularly interesting to investigate. To discuss how VOC and NO_x change affects ozone concentration, we rescaled the emissions of VOC and NO_x independently by increasing and decreasing 50% over Northern China (domain 2). Also, we doubled the isoprene emission factors in MEGAN biogenic emissions to increase the isoprene emissions and keep other emissions same as baseline as the concentration of isoprene is proved to be too low in the baseline. The emission changes were applied to the baseline scenario (R2) for the sensitivity studies has been summarized in Table 7 (by percentage).

4.1 Independent emission changes

Table 7. Changes in emissions by percentage applied to the baseline scenario (R2) for the sensitivity studies.

	Increased by	**Decreased by**
NO_x	+50%	+50%
VOC	+50%	-50%
Isoprene	+100%	-

Table 8. Comparison of hourly observed and simulated air pollutants in baseline and sensitivity runs at IAP in Beijing during 22-29 May 2017.

		Obs. Avg.	Sim. Avg.	Bias	RMSE	r
Baseline run	**O_3**	48.22	37.20	-11.02	30.36	0.70
	NO	6.07	5.07	-1.00	15.56	0.15
	NO_2	21.98	20.70	-1.28	16.06	0.14
	Aromatics	1.51	5.66	4.15	5.23	0.31
	ISO	0.52	0.22	-0.29	0.47	0.16
NOx emission +50%	**O_3**	48.22	27.39	-20.83	37.49	0.61
	NO	6.07	11.07	4.99	24.22	0.15
	NO_2	21.98	29.38	7.40	19.89	0.14
	Aromatics	1.51	5.82	4.30	5.39	0.32
	ISO	0.52	0.26	-0.26	0.45	0.16
NOx emission -50%	**O_3**	48.22	45.48	-2.74	28.44	0.70
	NO	6.07	1.10	-4.97	13.68	0.11
	NO_2	21.98	11.11	-10.87	17.38	0.12
	Aromatics	1.51	5.47	3.96	5.03	0.32
	ISO	0.52	0.20	-0.32	0.49	0.14
VOC emission +50%	**O_3**	48.22	41.46	-6.76	27.89	0.72
	NO	6.07	4.54	-1.54	15.08	0.15
	NO_2	21.98	20.60	-1.38	16.37	0.14
	Aromatics	1.51	8.36	6.85	8.29	0.31
	ISO	0.51	0.21	-0.31	0.48	0.15
VOC emission -50%	**O_3**	48.22	32.84	-15.38	34.28	0.64
	NO	6.07	5.65	-0.43	16.13	0.14
	NO_2	21.98	20.76	-1.23	15.76	0.14
	Aromatics	1.51	2.88	1.37	2.22	0.32
	ISO	0.51	0.25	-0.27	0.46	0.16

	O_3	48.22	38.16	-10.05	29.60	0.71
	NO	6.07	4.97	-1.10	15.51	0.15
ISO emission	**NO_2**	21.99	20.68	-1.31	16.14	0.14
factor +100%	**Aromatics**	1.51	5.66	4.14	5.21	0.31
	ISO	0.51	0.32	-0.19	0.42	0.27

Table 8 shows the effect on the simulation results of changing NOx or VOC emissions and Isoprene emission factors. We found that when adjusting NOx emissions, the concentration of NOx and ozone change significantly. When the emission of NOx increases by 50%, the average concentration of NO during simulation period increases about 120%, and the model further underestimates the average ozone concentration (Bias=-11.02 in baseline run, =-20.83 when increasing NOx emission by 50%). This can be explained by the fact that, without significant changes in VOC and isoprene concentrations, high NO concentration makes it easier for NO to participate in the direct removal of O_3. When NOx emission decreases by 50%, the bias of simulated and observed ozone concentration improved (Bias=-11.02 in baseline run, =-2.74 when increasing NOx emission by 50%), but the average of NO emission during simulation period decreases about 80%, which is far below the observation level. The simulation result of VOC concentration does not change significantly (less than 0.2 ppbv), and the concentration of isoprene is slightly changed (0.04 ppbv when NOx emission increases, and 0.02 ppbv when NOx emission decreases). Therefore, we focus on analysing the relationship between changes of ozone concentration and NOx emission. Correspondingly, the average concentration of aromatics during simulation period increase about 50%, and the performance of the model is better for ozone concentration (Bias=-11.02 in baseline run, =-6.76 when increasing VOC emission by 50%). When decreasing VOC by 50%, the average aromatics concentration decreases by 65%, and the bias in average ozone concentration becomes larger (Bias=-11.02 in baseline run, =-15.38 when decreasing VOC emission by 50%). The concentration of NO_2 did not change significantly when VOC emissions were changed. The concentration of NO is slightly changed (approximately 0.6 ppbv increase when VOC emission increases, and 0.5 ppbv decrease when NOx emission decreases). When doubling isoprene emissions, the isoprene

concentration increases about 45% and the ozone simulation improves a little bit (Bias=-11.02 in baseline run, =-10.05 when increasing isoprene emission factor by 100%), while simulated average concentrations of other chemicals show no significant difference.

a)

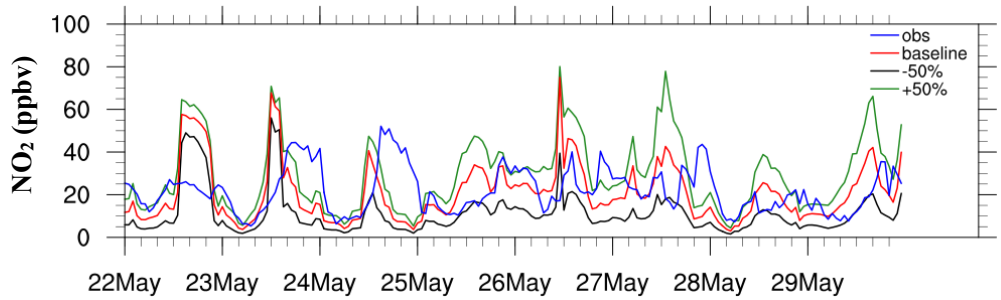

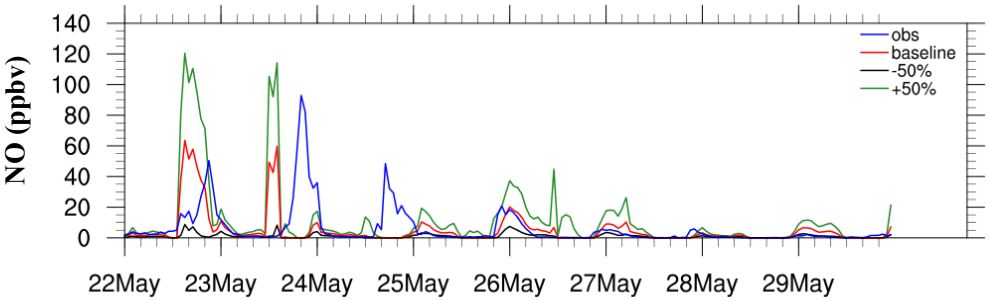

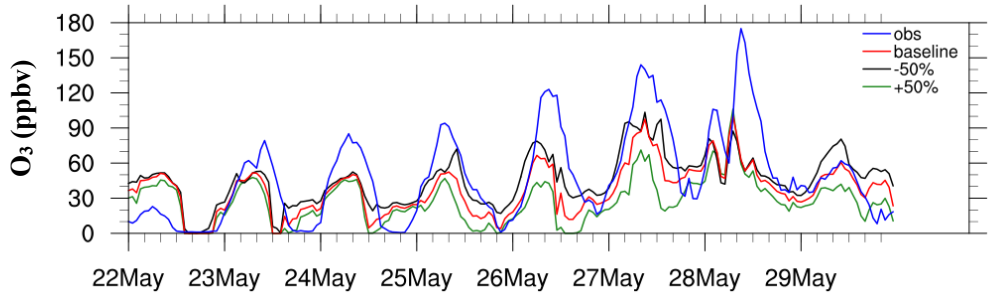

b)

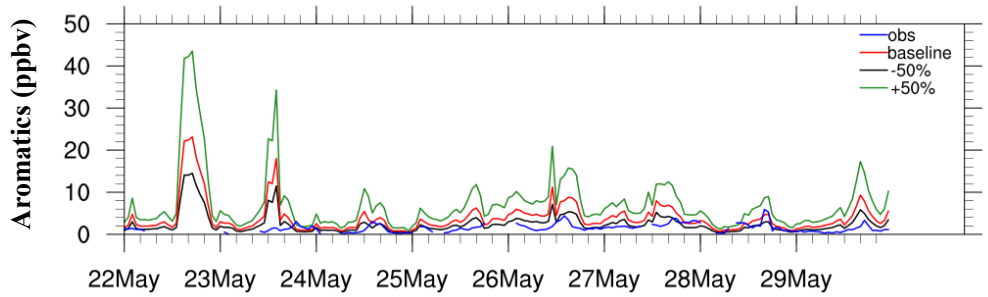

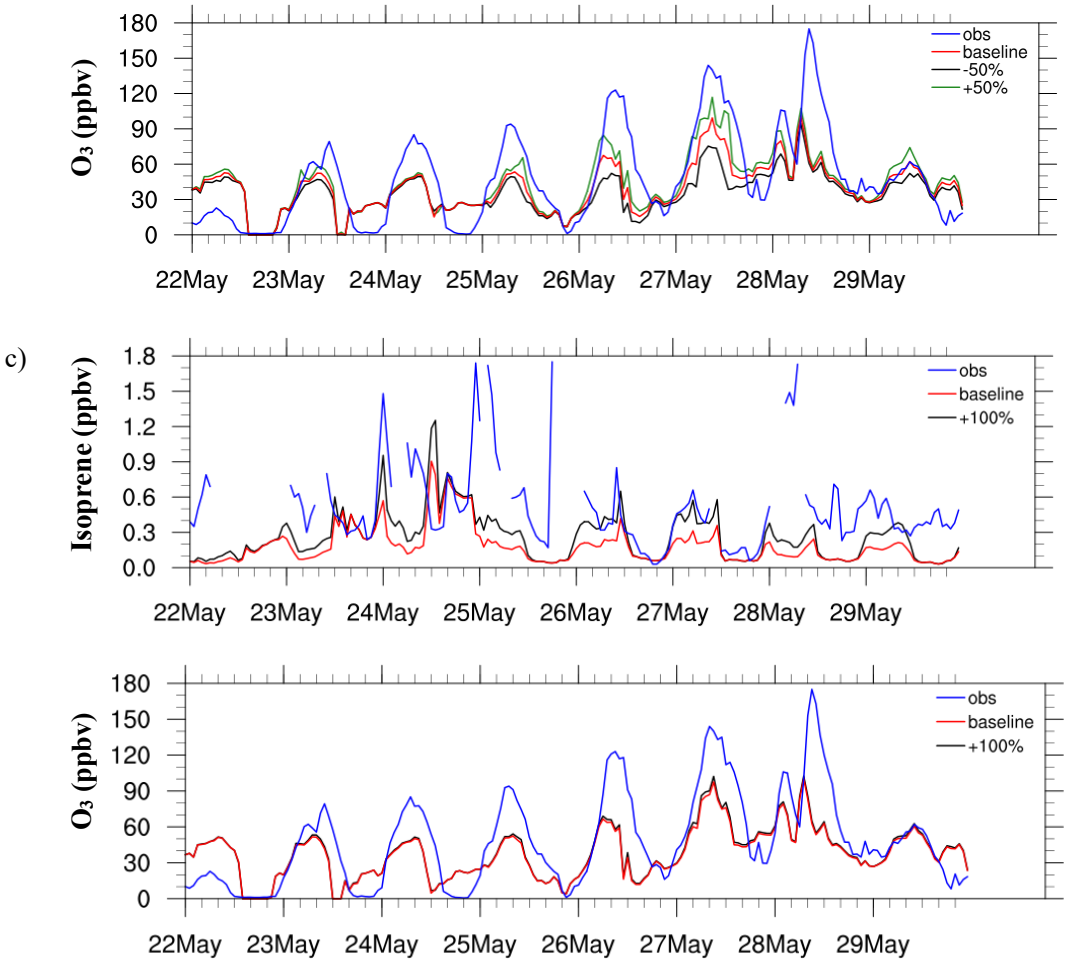

Figure 5. Concentrations of Ozone and a) NO_x timeseries at IAP, Beijing with NO_x emissions increased and decreased by 50%; b) VOC timeseries at IAP, Beijing with VOC emissions increased and decreased by 50%; c) isoprene timeseries at IAP, Beijing with isoprene emissions factor in biogenic emissions doubled.

Figure 5a presents the timeseries of NO_x and ozone concentration at IAP site when we changed the emissions of NO_x. Results show that increasing emissions of NO_x by 50% lowers the peak of daytime ozone concentration, and the simulated night-time ozone concentrations are also reduced to a fairly low level, which leads to further deviations compared with observations. This reflects that too much NOx inhibits the formation of ozone during daytime and enhances the consumption of ozone. When the emissions of NO_x are decreased by 50%, the simulating concentrations of daytime ozone are slightly increased, while the simulated lowest concentrations of ozone at night-time are increased. The difference between the

maximum and minimum daily ozone concentrations decreases, indicating that the effect of reducing NO_x on reducing night-time ozone removal is more significant than the effect of increasing ozone generation during the day. The results show that the effects of increasing or decreasing the emissions of NO_x by 50% to ozone simulations are relatively small, and comparison for NO_x concentration suggests that the emissions of NO_x applied in the baseline run performs better on simulating NO_x. Therefore, we suppose the emissions of NO_x should be kept the same as baseline run.

Figure 5b shows the timeseries of aromatics and ozone concentration at IAP site when we changed the emissions of VOC. We note that both increasing and decreasing VOC emissions by 50% affect the model's simulation of daytime peaks, but it has little effect on night-time low ozone concentrations compared with changing NO_x, suggesting the possible link between the simulation of aromatics and the significant underestimation of the peak of ozone concentration at daytime. The results show that the change of highest concentration level of ozone during the day is consistent with the emissions changes of VOC, even when the results show that model is still overestimates the concentration of aromatics. We note that, when the model overestimated the peaks of concentrations of aromatics, some species of aromatic which are not included in the observations may lead to the differences in total aromatic concentrations. In addition, there is also the possibility that other kinds of VOC which can affect the formation of ozone have been changed when changing the emissions of VOC, which may lead to the changes of ozone concentrations. For example, alkanes are very important for the formation of ozone, but we are unable to evaluate the model's simulation of alkanes due to the lack of corresponding observations. Considering only the effect of increasing or decreasing VOC emissions by 50% on the results, we suggest that increasing VOC by 50% is more helpful to improve ozone simulation.

Figure 5c presents the timeseries of isoprene and ozone concentration at IAP site when we doubled the emission factor of isoprene in biogenic emissions. Improvements in simulated isoprene concentration have been shown in the comparison between the run with doubled isoprene emission factor and the baseline. This may provide evidence confirming the conjecture that the land surface and vegetation may be not appropriate for central Beijing, underestimating

the existence and impact of vegetation there. However, changes in ozone concentration caused by isoprene is not significant, which may suggest that the model has difficulties in simulating the chemical process of ozone formation associated with isoprene.

4.2 Best emissions scenario

Previous sensitivity studies suggest that increased emissions of VOC by 50% can provide better ozone simulation results and increasing isoprene emission factors by 100% can improve isoprene simulation when ozone simulations have a little improvement, while increasing and decreasing NO_x emissions do not improve the ozone simulation as both increase the bias between simulation and observation. Based on the previous sensitivity studies, we performed an additional run with the best estimate of emission changes, with 50% increased VOC emissions and doubled isoprene emission factors. Table 9 shows the comparisons of the simulation of ozone, NO_x, VOC and isoprene between the observation, the baseline run and the run with the best emissions scenario. Results show that the model performance is better than in the baseline run (R2), which can be suggested by the bias between simulated and observed average ozone concentration (Bias=-11.02 in baseline run, =-5.89 with best emissions scenario) and the simulations of the ozone concentration peaks (Figure 6). This may be attributed to the increase of VOC emissions, where similar effects have been produced in the previous sensitivity study of increasing VOC emissions independently. When we only increase VOC by 50%, the bias of average ozone concentration is -6.76. In sensitivity run with best emission scenario, the bias further improves to -5.89, suggesting that doubling isoprene factor at the same time can bring a positive impact on ozone simulation. We also suspect from other studies (Ren et al., 2017; Chen et al., 2018b) that the isoprene in Beijing may be low, which provides a further justification on increasing isoprene emission by doubling isoprene emission factor.

Though improvements have been made in simulating ozone concentration by adjusting emissions, we note that there are still substantial differences which reflect weaknesses in the model and in the emissions. The bias of simulated and observed average ozone concentration still exists (bias = -5.89) and the model still underestimates the peaks of ozone (Figure 6) even though the VOC concentrations become much higher than observations by increasing VOC

emission. We speculate that this is still because the baseline VOC emissions are too low, or that the model underestimated the reactivities of VOC. Further investigations can be conducted on the VOC emissions and the reactivities of VOC in chemical reactions of ozone formation. The diurnal cycle of NOx cannot be well captured, which may be attributed to the wrong timing of emissions and with the timing of boundary layer mixing processes. The rush hour NO emissions after the boundary layer has collapsed may happen too soon in the model because the urban heat island isn't produced. And the night-time maximum in observed NOx may be due to diesel truck emissions which aren't in the inventory we use in the simulations. . In addition, the isoprene concentration is improved by doubling the isoprene emission factors in the biogenic emissions. But the isoprene concentration level still appears to be too low and the diurnal cycle also cannot be captured, which suggests that further improvement can be made on the land surface and the vegetation in Beijing, and its contributions to ozone formation in the model still need to be further investigated.

Table 9. Comparison of hourly observed and simulated air pollutants in best guess sensitivity run and baseline run at IAP in Beijing during 22-29 May 2017.

		Obs. Avg.	**Sim. Avg.**	**Bias**	**RMSE**	**r**
Baseline run	**O_3**	48.22	37.20	-11.02	30.36	0.70
	NO	6.07	5.07	-1.00	15.56	0.15
	NO_2	21.98	20.70	-1.28	16.06	0.14
	Aromatics	1.51	5.66	4.15	5.23	0.31
	ISO	0.52	0.22	-0.29	0.47	0.16
Best guess run	**O_3**	48.22	42.32	-5.89	27.42	0.73
	NO	6.07	4.45	-1.62	15.01	0.16
	NO_2	21.98	20.57	-1.42	16.44	0.14
	Aromatics	1.51	8.34	6.83	8.25	0.32
	ISO	0.51	0.29	-0.22	0.43	0.28

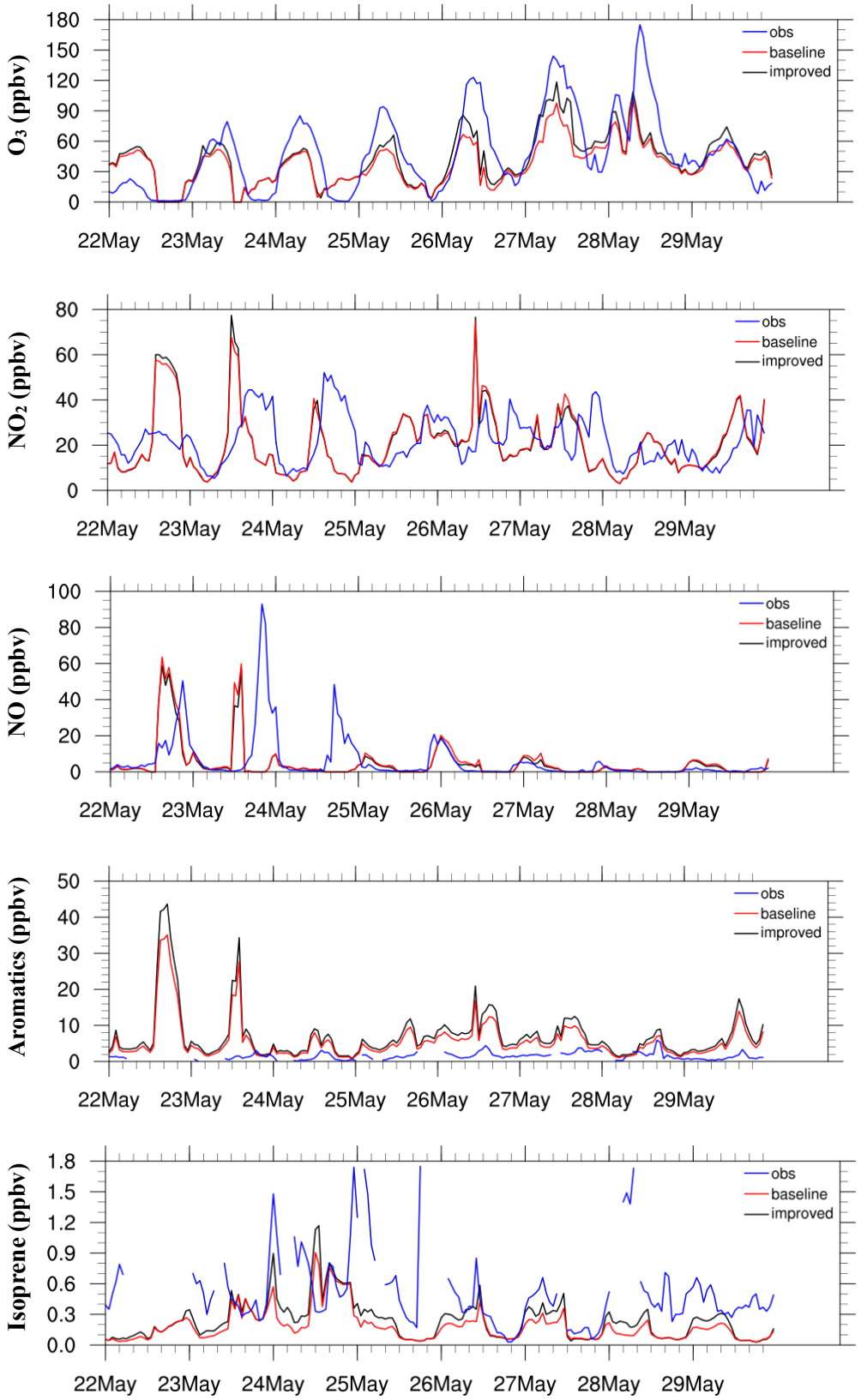

Figure 6. Concentrations of ozone, NO_2, NO, aromatics and isoprene timeseries at IAP, Beijing with VOC emissions increased by 50% and isoprene emissions factor in biogenic emissions doubled.

5. Conclusion

In this study, we applied WRF-Chem, a high-resolution nested air quality model, to simulate the air quality in North China from 15 May 2017 to 22 June 2017 and investigate the ozone and an ozone pollution event during this period by changing the emissions. We reproduce the meteorological parameters by capturing both the mean level and the variations using the model. We compare the effects of three different anthropogenic emissions scenarios on simulated air quality during the campaign period. We set the second full-period run (R2) as the baseline run in this study, because the simulation results of air pollutants from this run match observations better than the other full-period runs with different anthropogenic emissions scenarios (Bias=-10.19 at IAP, =-3.07 at 12-site, RMSE=28.74 at IAP, =21.86 at 12-site, smallest among three runs, r=0.68 at IAP, =0.74 at 12-site, biggest among three runs) , and it reproduces ozone concentration relatively well. We note that the NO_x and SO_2 are overestimated in the first run (R1) which uses the MEIC anthropogenic emissions for 2014, matching the results of emission changes studies (Zheng et al., 2018; Cheng et al., 2019) which indicate that emissions of NO_x and SO_2 decreased from 2014 to 2017, which inhibit the formation of ozone. Also, NO_x and SO_2 are underestimated in the third run (R3) which uses the MEIC anthropogenic emissions redistributed for 2017, leading to the suppressed consumption of ozone with NO_x as reactants at night-time. Therefore, ozone concentration in night-time is overestimated. A correlation of r=0.68 (r=0.74 at 12 sites) of ozone concentration and the timeseries at IAP site in Beijing comparing with observations suggests that the ozone concentration which is driven by the diurnal cycle can be well captured. We also note that there is an underestimation of the highest daily ozone concentrations. This may be attributed to the model's weakness in simulating VOC and isoprene. We speculate that some species of VOC may be incorrectly simulated and reproduced by the model. Isoprene concentration is underestimated in the model, which might because the land surface, vegetation and trees in Beijing are inappropriate.

We further performed sensitivity studies for a heavy ozone pollution period, investigating how emissions changes of NO_x, VOC and isoprene affects the simulation of ozone. Results show that doubling isoprene emission factors in biogenic emissions can improve the simulation of isoprene, suggesting that the emissions from tree coverage and vegetation are underestimated

by the land surface scheme in the model. We propose that adjustments to the land surface are needed to improve isoprene simulation as the isoprene concentration is underestimated. Increasing VOC emissions by 50% can improve the model's performance on simulating ozone, decreasing the underestimations of peaks of ozone concentrations in the polluted period though the comparison of simulated and observed aromatics show that the aromatics are overestimated. This may suggest that there may be important VOC emissions missing, or that the model underestimated the reactivities of VOC. After discussing sensitivity studies on emission changes of NO_x, VOC and isoprene, we get the emissions scenario with best performance on modelling ozone by increasing VOC by 50% and doubling isoprene emission factors. By investigating the best emissions scenario, our study demonstrates that ozone simulation has been improved as the bias, RMSE and correlations of ozone concentration are all improved compared with the baseline run. However, we still note that an underestimations in peak ozone concentrations still exists, which illustrates that the model's simulations of VOC still needed to be improved. We advise that further studies need to be done to resolve the ozone simulation problem by improving the VOC chemistry. Further research should focus on the emissions of more species of VOC and the balance between these species. Also, the reactivities of VOC in the process of ozone formation need to be analysed in more detail. The isoprene emission from biogenic sources needs to be improved by adjusting the land surface scheme, modifying the underestimation of tree coverage and vegetation in cities.

Reference

Ansari, T. U., Wild, O., Li, J., Yang, T., Xu, W., Sun, Y., and Wang, Z.: Effectiveness of short-term air quality emission controls: a high-resolution model study of Beijing during the Asia-Pacific Economic Cooperation (APEC) summit period, Atmos. Chem. Phys., 19, 8651–8668, https://doi.org/10.5194/acp-19-8651-2019, 2019.

Avnery, S., Mauzerall, D. L., Liu, J., Horowitz, L. W.: Global crop yield reductions due to surface ozone exposure: 1. Year 2000 crop production losses and economic damage. Atmospheric Environment, 45(13), 2284-2296, https://doi.org/10.1016/j.atmosenv.2010.11.045, 2011.

Bao, J. W., Michelson, S. A., Persson, P. O. G., Djalalova, I. V., and Wilczak, J. M.: Observed and WRF-simulated low-level winds in a high-ozone episode during the Central California Ozone Study. Journal of Applied Meteorology and Climatology, 47, 2372-2394, https://doi.org/10.1175/2008JAMC1822.1, 2008.

Bell, M., and Ellis, H.: Sensitivity analysis of tropospheric ozone to modified biogenic emissions for the Mid-Atlantic region, Atmos Environ, 38, 1879-1889, https://doi.org/10.1016/j.atmosenv.2004.01.012, 2004.

Brasseur, G., and Jacob, D.: Modeling of Atmospheric Chemistry. Cambridge: Cambridge University Press. doi:10.1017/9781316544754, 2017.

Brasseur, G., Orlannd, J. J., and Tyndal, G. S.: Atmospheric Chemistry and Global Change, Oxford University Press, New York, 1999.

Wallace, J., M., Hobbs, P., V.: Atmospheric science: an introductory survey. Elsevier, 2006.

Chen, F. and Dudhia, J.: Coupling an Advanced Land Surface-Hydrology Model with the Penn

State–NCAR MM5 Modeling System. Part II: Preliminary Model Validation, Mon. Weather Rev., 129, 587–604, https://doi.org/10.1175/1520-0493(2001)129<0569:CAALSH>2.0.CO;2, 2001

Chen, L., Guo, B., Huang, J. S., He, J., Wang, H. F., Zhang, S. Y., and Chen, S. X.: Assessing air-quality in Beijing-Tianjin-Hebei region: The method and mixed tales of PM2.5 and O_3, Atmos Environ, 193, 290-301, 2018a.

Chen, W., Tang, H., and Zhao, H.: Diurnal, weekly and monthly spatial variations of air pollutants and air quality of Beijing, Atmospheric Environment, 119, 21–34, https://doi.org/10.1016/j.atmosenv.2015.08.040, 2015.

Chen, W. H., Guenther, A. B., Wang, X. M., Chen, Y. H., Gu, D. S., Chang, M., Zhou, S. Z., Wu, L. L., and Zhang, Y. Q.: Regional to global biogenic isoprene emission responses to changes in vegetation from 2000 to 2015, J Geophys Res-Atmos, 123, 3757-3771, 10.1002/2017jd027934, 2018b.

Chen, Z., Xu, B., Cai, J., and Gao, B.: Understanding temporal patterns and characteristics of air quality in Beijing: A local and regional perspective, Atmos. Environ., 127, 303–315, https://doi.org/10.1016/j.atmosenv.2015.12.011, 2016.

Chen, Z., Zhuang, Y., Xie, X., Chen, D., Cheng, N., Yang, L., and Li, R.: Understanding long term variations of meteorological influences on ground ozone concentrations in Beijing during 2006-2016, Environ Pollut, 245, 29-37, 10.1016/j.envpol.2018.10.117, 2019

Cheng, J., Su, J., Cui, T., Li, X., Dong, X., Sun, F., Yang, Y., Tong, D., Zheng, Y., Li, Y., Li, J., Zhang, Q., and He, K.: Dominant role of emission reduction in $PM_{2.5}$ air quality improvement in Beijing during 2013–2017: a model-based decomposition analysis, Atmos. Chem. Phys., 19, 6125–6146, https://doi.org/10.5194/acp-19-6125-2019, 2019.

Cohen, A. J., Brauer, M., Burnett, R., Anderson, H. R., Frostad, J., Estep, K., et al.: Estimates and 25-year trends of the global burden of disease attributable to ambient air pollution: an analysis of data from the Global Burden of Diseases Study 2015. The Lancet, 389(10082), 1907-1918, https://doi.org/10.1016/S0140-6736(17)30505-6, 2017.

Duan, J. C., Tan, J. H., Yang, L., Wu, S., and Hao, J. M.: Concentration, sources and ozone formation potential of volatile organic compounds (VOCs) during ozone episode in Beijing, Atmos Res, 88, 25-35, https://doi.org/10.1016/j.atmosres.2007.09.004, 2008.

Emberson, L.D. ; Büker, P. ; Ashmore, M.R. ; Mills, G. ; Jackson, L.S. ; Agrawal, M. ; Atikuzzaman, M.D. ; Cinderby, S. ; Engardt, M. ; Jamir, C. ; Kobayashi, K. ; Oanh, N.T.K. ; Quadir, Q.F. ; Wahid, A.: A comparison of North American and Asian exposure–response data for ozone effects on crop yields. Atmospheric Environment, 43, 1945-1953, https://doi.org/10.1016/ j.atmosenv.2009.01.005, 2009.

Emmons, L. K., Walters, S., Hess, P. G., Lamarque, J.-F., Pfister, G. G., Fillmore, D., Granier, C., Guenther, A., Kinnison, D., Laepple, T., Orlando, J., Tie, X., Tyndall, G., Wiedinmyer, C., Baughcum, S. L., and Kloster, S.: Description and evaluation of the Model for Ozone and Related chemical Tracers, version 4 (MOZART-4), Geosci. Model Dev., 3, 43–67, https://doi.org/10.5194/gmd-3-43-2010, 2010.

Van Dingenen, R., Dentener, F. J., Raes, F., Krol, M. C., Emberson, L., & Cofala, J.: The global impact of ozone on agricultural crop yields under current and future air quality legislation. Atmospheric Environment, 43, 604-618, https://doi.org/10.1016/j.atmosenv. 2008.10.033, 2009.

Fast, J. D., Gustafson, W. I., Easter, R. C., Zaveri, R. A., Barnard, J. C., Chapman, E. G., Grell, G. A., and Peckham, S. E.: Evolution of ozone, particulates, and aerosol direct radiative forcing

in the vicinity of Houston using a fully coupled meteorology-chemistry- aerosol model, J. Geophys. Res.-Atmos., 111, 1–29, https://doi.org/10.1029/2005JD006721, 2006.

Finlayson-Pitts, B., and Pitts, James N.: Chemistry of the upper and lower atmosphere: Theory, experiments, and applications. Academic Press, https://doi.org/10.1016/B978-0-12-257060-5.X5000-X, 2000.

Fu, Y., and Liao, H.: Impacts of land use and land cover changes on biogenic emissions of volatile organic compounds in China from the late 1980s to the mid-2000s: Implications for tropospheric ozone and secondary organic aerosol, Tellus B: Chemical and Physical Meteorology, 66:1, https://doi.org/10.3402/tellusb.v66.24987, 2014.

Gao, W., Tie, X. X., Xu, J. M., Huang, R. J., Mao, X. Q., Zhou, G. Q., and Chang, L. Y.: Long-term trend of O_3 in a mega City (Shanghai), China: Characteristics, causes, and interactions with precursors, Sci. Total Environ., 603, 425–433, https://doi.org/10.1016/j.scitotenv.2017.06.099, 2017.

Geng, F., Zhao, C., Tang, X., Lu, G., and Tie, X.: Analysis of ozone and VOCs measured in Shanghai: A case study. Atmospheric Environment, 41(5), 989-1001, https://doi.org/10.1016/j.atmosenv.2006.09.023, 2007.

Grell, G. A., Peckham, S. E., Schmitz, R., McKeen, S. A., Frost, G., Skamarock, W. C., and Eder, B.: Fully coupled “online” chemistry within the WRF model. Atmospheric Environment, 39(37), 6957-6975, https://doi.org/10.1016/j.atmosenv.2005.04.027, 2005

Guenther, A. B., Jiang, X., Heald, C. L., Sakulyanontvittaya, T., Duhl, T., Emmons, L. K., and Wang, X.: The Model of Emissions of Gases and Aerosols from Nature version 2.1 (MEGAN2.1): an extended and updated framework for modelling biogenic emissions, Geosci. Model Dev., 5, 1471–1492, https://doi.org/10.5194/gmd-5-1471-2012, 2012.

Guenther, A., Karl, T., Harley, P., Wiedinmyer, C., Palmer, P. I., and Geron, C.: Estimates of global terrestrial isoprene emissions using MEGAN (Model of Emissions of Gases and Aerosols from Nature), Atmos. Chem. Phys., 6, 3181–3210, https://doi.org/10.5194/acp-6-3181-2006, 2006.

Guo, J., He, J., Liu, H., Miao, Y., Liu, H., and Zhai, P.: Impact of various emission control schemes on air quality using WRF-Chem during APEC China 2014. Atmospheric Environment, 140, 311-319, https://doi.org/10.1016/j.atmosenv.2016.05.046, 2016

Hong, S.-Y., Noh, Y., and Dudhia, J.: A New Vertical Diffusion Package with an Explicit Treatment of Entrainment Processes, Mon. Weather Rev., 134, 2318–2341, https://doi.org/10.1175/MWR3199.1, 2006.

Hu, J., Chen, J., Ying, Q., and Zhang, H.: One-year simulation of ozone and particulate matter in China using WRF/CMAQ modeling system, Atmos. Chem. Phys., 16, 10333–10350, https://doi.org/10.5194/acp-16-10333-2016, 2016.

Jacob, D., J.: Introduction to atmospheric chemistry. Princeton University Press, 1999.

Jiang, G., and Fast, J. D.: Modeling the effects of VOC and NOx emission sources on ozone formation in Houston during the TexAQS 2000 field campaign. Atmospheric Environment, 38(30), 5071-5085, https://doi.org/10.1016/j.atmosenv.2004.06.012, 2004.

Kitayama, K., Morino, Y., Yamaji, K., and Chatani, S.: Uncertainties in O_3 concentrations simulated by CMAQ over Japan using four chemical mechanisms. Atmospheric environment, 198, 448-462, https://doi.org/10.1016/j.atmosenv.2018.11.003, 2019.

Li, J., Wang, Z., Akimoto, H., Yamaji, K., Takigawa, M., Pochanart, P., Liu, Y., Tanimoto, H.,

and Kanaya, Y.: Near-ground ozone source attributions and outflow in central eastern China during MTX2006, Atmos. Chem. Phys., 8, 7335-7351, https://doi.org/10.5194/acp-8-7335-2008, 2008.

Li, J., Yang, W., Wang, Z., Chen, H., Hu, B., Li, J., Sun, Y., Fu, P., and Zhang, Y.: Modeling study of surface ozone source-receptor relationships in East Asia. Atmospheric research, 167, 77-88, https://doi.org/10.1016/j.atmosres.2015.07.010, 2016

Li, K., Jacob, D. J., Liao, H., Shen, L., Zhang, Q., and Bates, K. H.: Anthropogenic drivers of 2013–2017 trends in summer surface ozone in China. Proceedings of the National Academy of Sciences, 116(2), 422-427, https://doi.org/10.1073/pnas.1812168116, 2019a.

Li, M., Liu, H., Geng, G., Hong, C., Liu, F., Song, Y., Tong, D., Zheng, B., Cui H., Man, H., Zhang, Q., and He, K.: Anthropogenic emission inventories in China: a review, National Science Review, 4, 834-866, 2017.

Li, M., Zhang, Q., Streets, D. G., He, K. B., Cheng, Y. F., Emmons, L. K., Huo, H., Kang, S. C., Lu, Z., Shao, M., Su, H., Yu, X., and Zhang, Y.: Mapping Asian anthropogenic emissions of non-methane volatile organic compounds to multiple chemical mechanisms, Atmos. Chem. Phys., 14, 5617-5638, https://doi.org/10.5194/acp-14-5617-2014, 2014.

Li, M., Zhang, Q., Zheng, B., Tong, D., Lei, Y., Liu, F., Hong, C., Kang, S., Yan, L., Zhang, Y., Bo, Y., Su, H., Cheng, Y., and He, K.: Persistent growth of anthropogenic non-methane volatile organic compound (NMVOC) emissions in China during 1990–2017: drivers, speciation and ozone formation potential, Atmos. Chem. Phys., 19, 8897–8913, https://doi.org/10.5194/acp-19-8897-2019, 2019b.

Liu, Z., Wang, Y., Gu, D., Zhao, C., Huey, L. G., Stickel, R., Liao, J., Shao, M., Zhu, T., Zeng, L., Amoroso, A., Costabile, F., Chang, C.-C., and Liu, S.-C.: Summertime photochemistry

during CAREBeijing-2007: ROx budgets and O_3 formation, Atmos. Chem. Phys., 12, 7737-7752, https://doi.org/10.5194/acp-12-7737-2012, 2012.

Lu, X., Hong, J. Y., Zhang, L., Cooper, O. R., Schultz, M. G., Xu, X. B., Wang, T., Gao, M., Zhao, Y. H., and Zhang, Y. H.: Severe surface ozone pollution in China: A global perspective, Environ Sci Tech Let, 5, 487-494, https://doi.org/10.1021/acs.estlett.8b00366, 2018.

Lyu, X., Wang, N., Guo, H., Xue, L., Jiang, F., Zeren, Y., Cheng, H., Cai, Z., Han, L., and Zhou, Y.: Causes of a continuous summertime O_3 pollution event in Jinan, a central city in the North China Plain, Atmos. Chem. Phys., 19, 3025–3042, https://doi.org/10.5194/acp-19-3025-2019, 2019.

Ma, M., Gao, Y., Wang, Y., Zhang, S., Leung, L. R., Liu, C., Wang, S., Zhao, B., Chang, X., Su, H., Zhang, T., Sheng, L., Yao, X., Gao, H.: Substantial ozone enhancement over the North China Plain from increased biogenic emissions due to heat waves and land cover in summer 2017. Atmos. Chem. Phys. Discuss. 27, 1680-7375, https://doi.org/10.5194/acp-2019-362, 2019.

Ma, Z., Xu, J., Quan, W., Zhang, Z., Lin, W., and Xu, X.: Significant increase of surface ozone at a rural site, north of eastern China, Atmos. Chem. Phys., 16, 3969–3977, https://doi.org/10.5194/acp-16-3969-2016, 2016.

Michalakes, J., Chen, S., Dudhia, J., Hart, L., Klemp, J., Middlecoff, J., and Skamarock, W.: Development of a next-generation regional weather research and forecast model. In Developments in Teracomputing, 269-276, https://doi.org/10.1142/9789812799685_0024, 2001.

Mlawer, E. J., Taubman, S. J., Brown, P. D., Iacono, M. J., and Clough, S. A.: Radiative transfer for inhomogeneous atmospheres: RRTM, a validated correlated-k model for the longwave, J.

Geophys. Res., 102, 16663, https://doi.org/10.1029/97JD00237, 1997.

Monks, P. S., Archibald, A. T., Colette, A., Cooper, O., Coyle, M., Derwent, R., Fowler, D., Granier, C., Law, K. S., Mills, G. E., Stevenson, D. S., Tarasova, O., Thouret, V., von Schneidemesser, E., Sommariva, R., Wild, O., and Williams, M. L.: Tropospheric ozone and its precursors from the urban to the global scale from air quality to short-lived climate forcer, Atmos. Chem. Phys., 15, 8889–8973, https://doi.org/10.5194/acp-15-8889-2015, 2015.

Naeem, S., Cao, C., Fatima, K., Najmuddin, O., and Acharya, B.: Landscape greening policies-based land use/land cover simulation for Beijing and Islamabad—An implication of sustainable urban ecosystems. Sustainability, 10(4), 1049, https://doi.org/10.3390/su10041049, 2018.

Pu, X., Wang, T. J., Huang, X., Melas, D., Zanis, P., Papanastasiou, D. K., and Poupkou, A.: Enhanced surface ozone during the heat wave of 2013 in Yangtze River Delta region, China, Sci Total Environ, 603, 807-816, https://doi.org/10.1016/j.scitotenv.2017.03.056, 2017.

Ren, Y., Qu, Z. L., Du, Y. Y., Xu, R. H., Ma, D. P., Yang, G. F., Shi, Y., Fan, X., Tani, A., Guo, P. P., Ge, Y., and Chang, J.: Air quality and health effects of biogenic volatile organic compounds emissions from urban green spaces and the mitigation strategies, Environ Pollut, 230, 849-861, https://doi.org/10.1016/j.envpol.2017.06.049, 2017.

Safieddine, S., Boynard, A., Coheur, P.-F., Hurtmans, D., Pfister, G., Quennehen, B., Thomas, J. L., Raut, J.-C., Law, K. S., Klimont, Z., Hadji-Lazaro, J., George, M., and Clerbaux, C.: Summertime tropospheric ozone assessment over the Mediterranean region using the thermal infrared IASI/MetOp sounder and the WRF-Chem model, Atmos. Chem. Phys., 14, 10119-10131, https://doi.org/10.5194/acp-14-10119-2014, 2014.

Shi, Z., Vu, T., Kotthaus, S., Harrison, R. M., Grimmond, S., Yue, S., Zhu, T., Lee, J., Han, Y., Demuzere, M., Dunmore, R. E., Ren, L., Liu, D., Wang, Y., Wild, O., Allan, J., Acton, W. J.,

Barlow, J., Barratt, B., Beddows, D., Bloss, W. J., Calzolai, G., Carruthers, D., Carslaw, D. C., Chan, Q., Chatzidiakou, L., Chen, Y., Crilley, L., Coe, H., Dai, T., Doherty, R., Duan, F., Fu, P., Ge, B., Ge, M., Guan, D., Hamilton, J. F., He, K., Heal, M., Heard, D., Hewitt, C. N., Hollaway, M., Hu, M., Ji, D., Jiang, X., Jones, R., Kalberer, M., Kelly, F. J., Kramer, L., Langford, B., Lin, C., Lewis, A. C., Li, J., Li, W., Liu, H., Liu, J., Loh, M., Lu, K., Lucarelli, F., Mann, G., McFiggans, G., Miller, M. R., Mills, G., Monk, P., Nemitz, E., O'Connor, F., Ouyang, B., Palmer, P. I., Percival, C., Popoola, O., Reeves, C., Rickard, A. R., Shao, L., Shi, G., Spracklen, D., Stevenson, D., Sun, Y., Sun, Z., Tao, S., Tong, S., Wang, Q., Wang, W., Wang, X., Wang, X., Wang, Z., Wei, L., Whalley, L., Wu, X., Wu, Z., Xie, P., Yang, F., Zhang, Q., Zhang, Y., Zhang, Y., and Zheng, M.: Introduction to the special issue “In-depth study of air pollution sources and processes within Beijing and its surrounding region (APHH-Beijing)”, Atmos. Chem. Phys., 19, 7519–7546, https://doi.org/10.5194/acp-19-7519-2019, 2019.

Sillman, S.: The relation between ozone, NOx and hydrocarbons in urban and polluted rural environments, Atmos Environ, 33, 1821-1845, https://doi.org/10.1016/S1352-2310(98)00345-8, 1999.

Skamarock, W. C., Klemp, J. B., Dudhia, J., Gill, D. O., Barker, D. M., Duda, M. G., Huang, X.-Y., Wang, W., and Powers, J. G.: A Description of the Advanced Research WRF Version 3. NCAR Tech. Note NCAR/TN-475+STR, 113 pp. https://doi.org/10.5065/D68S4MVH, 2008.

Song, J., Lei, W., Bei, N., Zavala, M., de Foy, B., Volkamer, R., Cardenas, B., Zheng, J., Zhang, R., and Molina, L. T.: Ozone response to emission changes: a modeling study during the MCMA-2006/MILAGRO Campaign, Atmos. Chem. Phys., 10, 3827-3846, https://doi.org/10.5194/acp-10-3827-2010, 2010.

Soriano, J. B., Abajobir, A. A., Abate, K. H., Abera, S. F., Agrawal, A., Ahmed, M. B., et al.: Global, regional, and national deaths, prevalence, disability-adjusted life years, and years lived with disability for chronic obstructive pulmonary disease and asthma, 1990–2015: a systematic

analysis for the Global Burden of Disease Study 2015. The Lancet Respiratory Medicine, 5(9), 691-706, https://doi.org/10.1016/S2213-2600(17)30293-X, 2017.

Stavrakou, T., Müller, J.-F., Bauwens, M., De Smedt, I., Van Roozendael, M., Guenther, A., Wild, M., and Xia, X.: Isoprene emissions over Asia 1979–2012: impact of climate and land-use changes, Atmos. Chem. Phys., 14, 4587-4605, https://doi.org/10.5194/acp-14-4587-2014, 2014.

Sun, L., Xue, L., Wang, T., Gao, J., Ding, A., Cooper, O. R., Lin, M., Xu, P., Wang, Z., Wang, X., Wen, L., Zhu, Y., Chen, T., Yang, L., Wang, Y., Chen, J., and Wang, W.: Significant increase of summertime ozone at Mount Tai in Central Eastern China, Atmos. Chem. Phys., 16, 10637–10650, https://doi.org/10.5194/acp-16-10637-2016, 2016.

Sun, L., Xue, L., Wang, Y., Li, L., Lin, J., Ni, R., Yan, Y., Chen, L., Li, J., Zhang, Q., and Wang, W.: Impacts of meteorology and emissions on summertime surface ozone increases over central eastern China between 2003 and 2015, Atmos. Chem. Phys., 19, 1455–1469, https://doi.org/10.5194/acp-19-1455-2019, 2019.

Tie, X., Brasseur, G., and Ying, Z.: Impact of model resolution on chemical ozone formation in Mexico City: application of the WRF-Chem model, Atmos. Chem. Phys., 10, 8983-8995, https://doi.org/10.5194/acp-10-8983-2010, 2010.

Tie, X., Geng, F., Guenther, A., Cao, J., Greenberg, J., Zhang, R., Apel, E., Li, G., Weinheimer, A., Chen, J., and Cai, C.: Megacity impacts on regional ozone formation: observations and WRF-Chem modeling for the MIRAGE-Shanghai field campaign, Atmos. Chem. Phys., 13, 5655–5669, https://doi.org/10.5194/acp-13-5655-2013, 2013.

Tie, X., Geng, F., Peng, L., Gao, W., and Zhao, C.: Measurement and modeling of O_3 variability in Shanghai, China: Application of the WRF-Chem model. Atmospheric Environment, 43,

4289-4302, https://doi.org/10.1016/j.atmosenv.2009.06.008, 2009.

Tie, X., Madronich, S., Li, G., Ying, Z., Zhang, R., Garcia, A. R., Lee-Taylor, J., and Liu, Y.: Characterizations of chemical oxidants in Mexico City: A regional chemical dynamical model (WRF-Chem) study. Atmospheric Environment, 41(9), 1989-2008, https://doi.org/10.1016/j.atmosenv.2006.10.053, 2007

Tuccella, P., Curci, G., Visconti, G., Bessagnet, B., Menut, L., Park, R. J.: Modeling of gas and aerosol with WRF/Chem over Europe: Evaluation and sensitivity study. Journal of Geophysical Research: Atmospheres, 117, https://doi.org/10.1029/2011JD016302, 2012.

Vieno, M., Dore, A. J., Stevenson, D. S., Doherty, R., Heal, M. R., Reis, S., Hallsworth, S., Tarrason, L., Wind, P., Fowler, D., Simpson, D., and Sutton, M. A.: Modelling surface ozone during the 2003 heat-wave in the UK, Atmos. Chem. Phys., 10, 7963-7978, https://doi.org/10.5194/acp-10-7963-2010, 2010.

Wang, J., Wang, S., Jiang, J., Ding, A., Zheng, M., Zhao, B., Wong D. C., Zhou W., Zheng G., Wang L., Pleim, J. E., and Hao J.: Impact of aerosol–meteorology interactions on fine particle pollution during China's severe haze episode in January 2013. Environmental Research Letters, 9(9), 094002. http://doi.org/10.1088/1748-9326/9/9/094002, 2014.

Wang, Q. G., Han, Z. W., Wang, T. J., and Zhang, R. J.: Impacts of biogenic emissions of VOC and NOx on tropospheric ozone during summertime in eastern China, Sci Total Environ, 395, 41-49, https://doi.org/10.1016/j.scitotenv.2008.01.059, 2008.

Wiedinmyer, C., Akagi, S. K., Yokelson, R. J., Emmons, L. K., Al-Saadi, J. A., Orlando, J. J., and Soja, A. J.: The Fire Inventory from NCAR (FINN): a high resolution global model to estimate the emissions from open burning, Geosci. Model Dev., 4, 625– 641, https://doi.org/10.5194/gmd-4-625-2011, 2011.

Wild, O., Zhu, X., and Prather, M. J.: Fast-J: Accurate simulation of in- and below-cloud photolysis in tropospheric chemical models, J. Atmos. Chem., 37, 245–282, https://doi.org/10.1023/A:1006415919030, 2000.

Wu, J., Wang, Q., Chen, H., Zhang, Y., and Wild, O.: On the origin of surface ozone episode in Shanghai over Yangtze River Delta during a prolonged heat wave. Aerosol and Air Quality Research, 17(11), 2804-2815, https://doi.org/10.4209/aaqr.2017.03.0101, 2017.

Xing, J., Wang, S. X., Jang, C., Zhu, Y., and Hao, J. M.: Nonlinear response of ozone to precursor emission changes in China: a modeling study using response surface methodology, Atmos. Chem. Phys., 11, 5027-5044, https://doi.org/10.5194/acp-11-5027-2011, 2011.

Xu, J., Tie, X., Gao, W., Lin, Y., and Fu, Q.: Measurement and model analyses of the ozone variation during 2006 to 2015 and its response to emission change in megacity Shanghai, China, Atmos. Chem. Phys., 19, 9017–9035, https://doi.org/10.5194/acp-19-9017-2019, 2019.

Zaveri, R. A. and Peters, L. K.: A new lumped structure photochemical mechanism for large-scale applications, J. Geophys. Res., 104, 30387, https://doi.org/10.1029/1999JD900876, 1999.

Zaveri, R. A., Easter, R. C., Fast, J. D., and Peters, L. K.: Model for Simulating Aerosol Interactions and Chemistry (MOSAIC), J. Geophys. Res., 113, D13204, https://doi.org/10.1029/2007JD008782, 2008.

Zhang, J., Gao, Y., Luo, K., Leung, L. R., Zhang, Y., Wang, K., and Fan, J.: Impacts of compound extreme weather events on ozone in the present and future, Atmos. Chem. Phys., 18, 9861–9877, https://doi.org/10.5194/acp-18-9861-2018, 2018.

Zhang, L., Wang, T., Lv, M., and Zhang, Q.: On the severe haze in Beijing during January 2013:

Unraveling the effects of meteorological anomalies with WRF-Chem. Atmospheric Environment, 104, 11-21, https://doi.org/10.1016/j.atmosenv.2015.01.001, 2015

Zhang, Q., Yuan, B., Shao, M., Wang, X., Lu, S., Lu, K., Wang, M., Chen, L., Chang, C.-C., and Liu, S. C.: Variations of ground-level O_3 and its precursors in Beijing in summertime between 2005 and 2011, Atmos. Chem. Phys., 14, 6089-6101, https://doi.org/10.5194/acp-14-6089-2014, 2014.

Zhao, Y., Sun, R., and Ni, Z.: Identification of Natural and Anthropogenic Drivers of Vegetation Change in the Beijing-Tianjin-Hebei Megacity Region. Remote Sensing, 11(10), 1224, https://doi.org/10.3390/rs11101224, 2019.

Zheng, B., Tong, D., Li, M., Liu, F., Hong, C., Geng, G., Li, H., Li, X., Peng, L., Qi, J., Yan, L., Zhang, Y., Zhao, H., Zheng, Y., He, K., and Zhang, Q.: Trends in China's anthropogenic emissions since 2010 as the consequence of clean air actions, Atmos. Chem. Phys., 18, 14095–14111, https://doi.org/10.5194/acp-18-14095-2018, 2018.